# Paul Scherrer Institut, CH-5232 Villigen, Switzerland

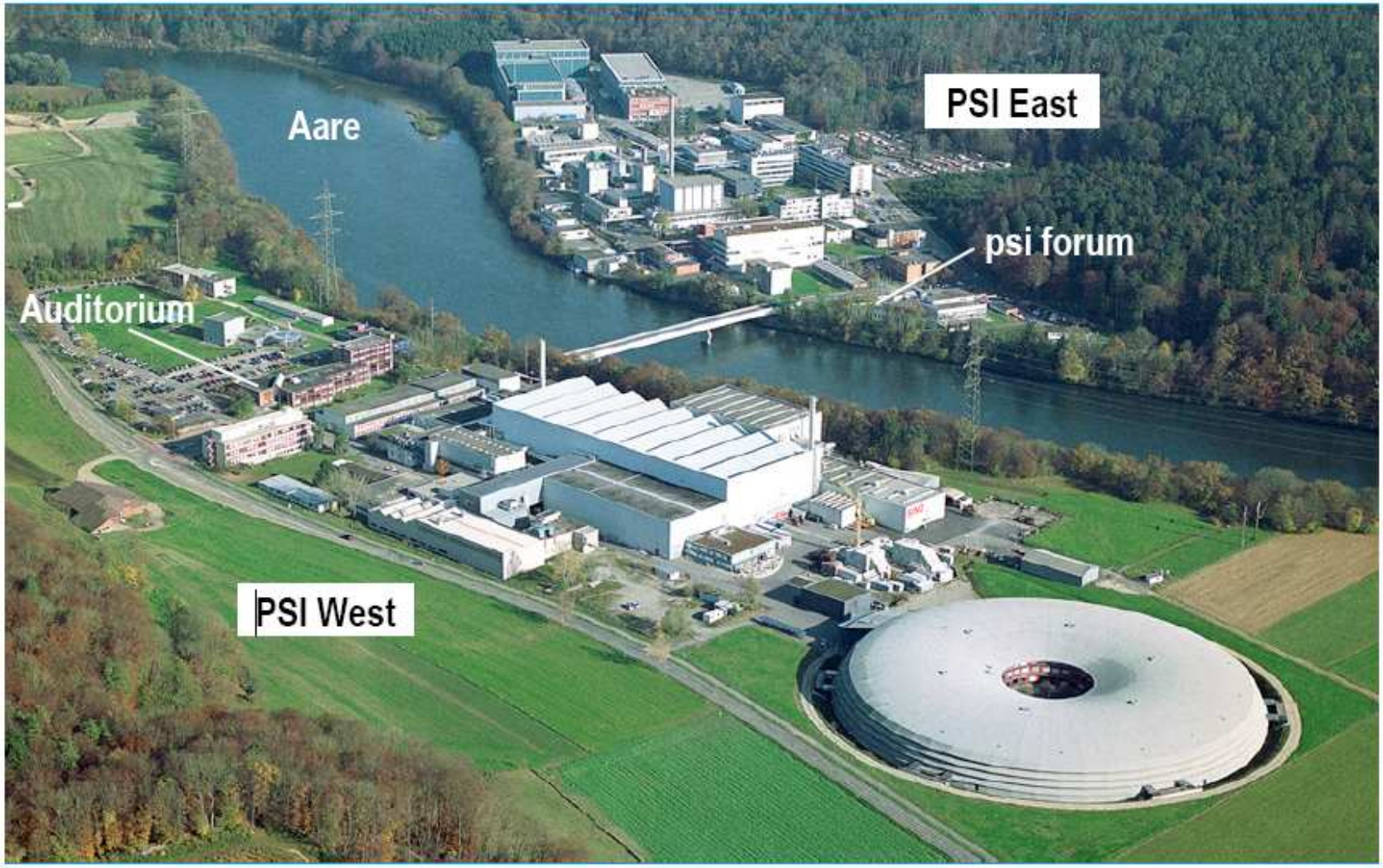


≪ WIR SCHAFFEN WISSEN - HEUTE FÜR MORGEN ≫

# Non-Equilibrium Dynamics Studied by Femtosecond Laser-Pump/X-Ray Probe Diffraction

**G. Ingold**

**FEMTO Group**

**Paul Scherrer Institut**

**Laboratory for Synchrotron Radiation**

**Cheiron School 2011**

**SPring-8, Japan**

**Sep 25 - Oct 5, 2011**

# Motivation

## Dynamics, Correlations and Coupling in Ultrafast Phase Transitions in Condensed Matter:

## Transition from microscopic to macroscopic behaviour

# Bibliography I


## • Non-resonant (grazing incidence) diffraction

- **S. L. Johnson et al.,** *Non-equilibrium phonon dynamics studied by grazing-incidence femtosecond X-ray crystallography*, **Acta Cryst. A66 (2010) 157.**

- **I. K. Robinson and D. J. Tweet,** *Surface x-ray diffraction*, **Rep. Prog. Phys. 55 (1992) 599.**

## • Resonant diffraction

- **M. Altarelli,** *Resonant X-ray Scattering: A Theoretical Introduction*, **Lect. Notes Phys. 697 (2006) 201, Springer**

- **S. W. Lovesey et al.,** *Electronic properties of crystalline materials observed in X-ray diffraction*, **Physics Reports 411 (2005) 233.**

- **J. P. Hill and D.F. McMorrow,** *X-ray Resonant Exchange Scattering: Polarization Dependence and Correlation Functions*, **Acta Cryst. A52 (1996) 236.**

- **S. W. Lovesey and S. P. Collins,** *X-Ray Scattering and Absorption by Magnetic Materials*, **Clarendon Press, Oxford, (1996).**

## • Strongly correlated systems:

- **Y. Tokura,** *Critical features of colossal magnetoresistive manganites*, **Rep. Prog. Phys. 69 (2006) 797.**

- **E. Dagotto et al.,** *Colossal Magnetoresistant Materials: The Key Role of Phase Separation*, **Physics Reports 344 (2001) 1.**

- **M. Imada, A. Fujimori and Y. Tokura** *Metal-insulator transitions*, **Rev. Mod. Phys. 70 (1998) 1039.**

## • Magnetization dynamics

- **A. Kirilyuk et al.,** *Ultrafast optical manipulation of magnetic order*, **Rev. Mod. Phys. 82 (2010) 2731.**

# Bibliography II

## • Inelastic X-ray scattering


- **P. Abbamonte et al.,** *Ultrafast Imaging and the Phase Problem for Inelastic X-Ray Scattering*, **Adv. Mater. 22 (2010) 1141.**

- **J.P. Reed et al.,** *The Effective Fine- Structure Constant of Freestanding Graphene Measured in Graphite*, **Science 330 (2010) 805.**

- **P. Abbamonte et al.,** *Implicit spatial averaging in inversion of inelastic x-ray scattering data*, **Phys. Rev. B 80 (2009) 054302.**


## • Multiferroics


- **K. W. Wang et al.,** *Multiferroicity: the coupling between magnetic and polarization orders*, **Advances in Physics 5 (2009) 321.**

- **D. Khomskii,** *Classifying multiferroics: Mechanisms and effects*, **Physics 2 (2009)**

- **J. van den Bring and D. Khomskii,** *Review Article: Multiferroicity due to charge ordering*, **J. Phys.: Condens. Matter 20 (2008) 434217.**

- **S.-W. Cheong and M. Mostovoy,** *Multiferroics: a magnetic twist for ferroelectricity*, **Nature Materials 6 (2007) 13.**

- **H.C. Walker et al.,** *Femtoscale Magnetically Induced Lattice Distortions in Multiferroic* $TbMnO_3$, **Science 333 (2007) 1273.**

# Ballet dancing: choreography of complex motion




[ photos: www.staatsballett-berlin.de ]

**... coordinated motion due to mutual vision and musical rhythm ...**

# Biology: the formation process vast oceanic fish shoals


[figures: www.seatops.com] [N. Markis et al., Science 323 (2009)]

- In the beginning the fish are widely distributed in a diffuse low-density layer close to seafloor
- Shoal formation is triggered by reduction in light level (external stimulus)
- Shoals evolve from small, isolated catalyzing clusters to extensive, dense horizontal layers
- Having reached a critical population density, coherent shoal-forming waves appear
- Vast shoals migrate by synchronous swimming of hundreds of millions of individual fish
- Vast shoals remain stable in the night and dissipate as light levels increase with sunrise

# Choreography: timescale of coherent motion

**Ballet dancing: $\sim 10^{-2}$ - $10^{1}$ s**

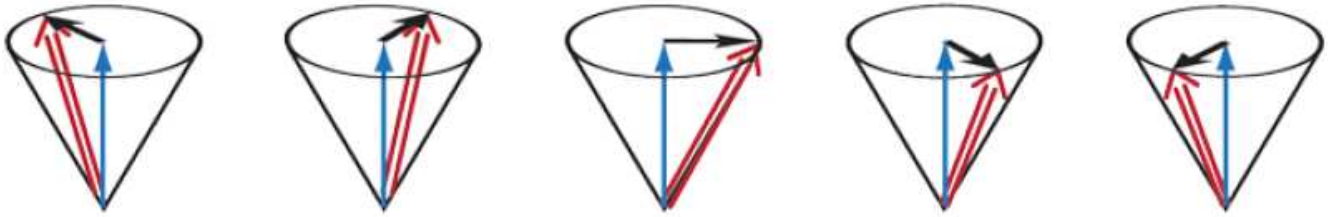

**Spin wave (magnon) excitation: $\sim 10^{-13}$ - $10^{12}$ s**

# Correlated Structural and Electronic Dynamics in Complex Materials

**Goal: Resolve correlated dynamics: lattice, charge, orbital and spin order**
**real time & atomic resolution**

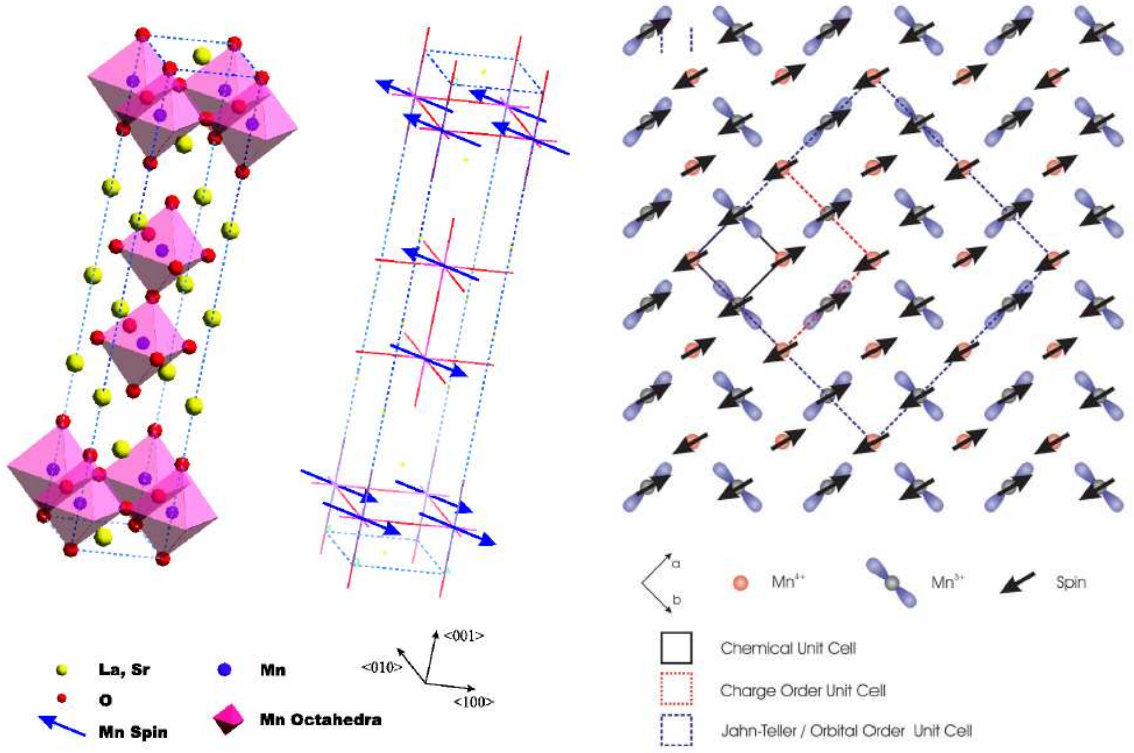


- **Lattice dynamics:** (time domain & atomic resolution): $\tau_{vib} \simeq$ 100 fs (vibrational period)
- **Electron dynamics:** (charge-, orbital-, spin-order): $\tau_{e-ph} \simeq$ 1 ps (e-phonon);
  $\tau_{e-e} \simeq$ 10 fs (e-e scattering); $\tau_{e-corr} \simeq$ 0.1 fs (e-correlation)

**... warning: even simple mechanical systems exhibit complex behaviour depending on the boundary conditions ...**


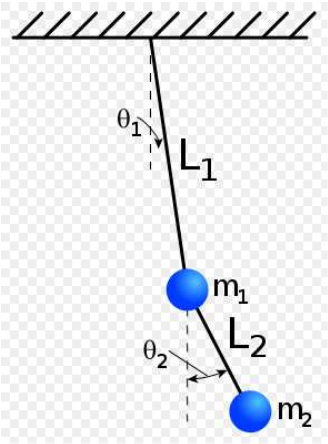


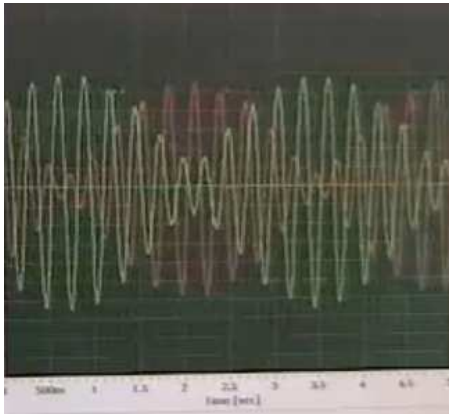

**Coupled Pendula**

**regular motion**

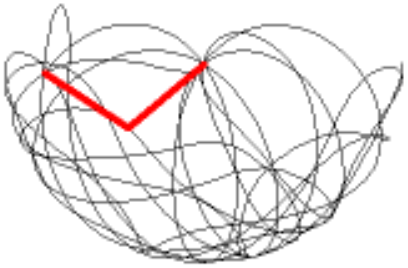

**Double Pendula**

**chaotic motion**

**This lecture is mainly about our R & D work**

**- work in progress -**

# Laser-pump / X-ray-probe Experiments

# Femtosecond Probing of Long-Range Order in Solids with Non-resonant and Resonant X-Ray Scattering

# Outline of the lecture

- **Motivation**
- **Why study strongly correlated systems & perovskite structure ?**
- **Short remark: stimulated non-equilibrium phase transition**
- **All optical pump-probe: reflectivity & TR-MOKE**
- **Femtosecond X-rays generated with undulators & relativistic electron beams**

  **( generation at slicing sources & XFELs, synchronization, timing )**
- **Femtosecond grazing incidence X-ray diffraction**

  **( experimental set-up & technique, coherent phonon dynamics )**
- **Laser-pump / X-ray-probe: hard X-rays**

  **( Slicing source: non-resonant diffraction on manganites )**
- **Laser-pump / X-ray-probe: soft X-rays**

  **( Free electron laser : resonant diffraction on multiferroics )**
- **Summary & conclusions**

# Why strongly correlated systems & perovskite structure ?

## Effective One-Particle Approach ⇔ Electronic Correlations

**Dynamics is becoming accessible by DMFT theories**

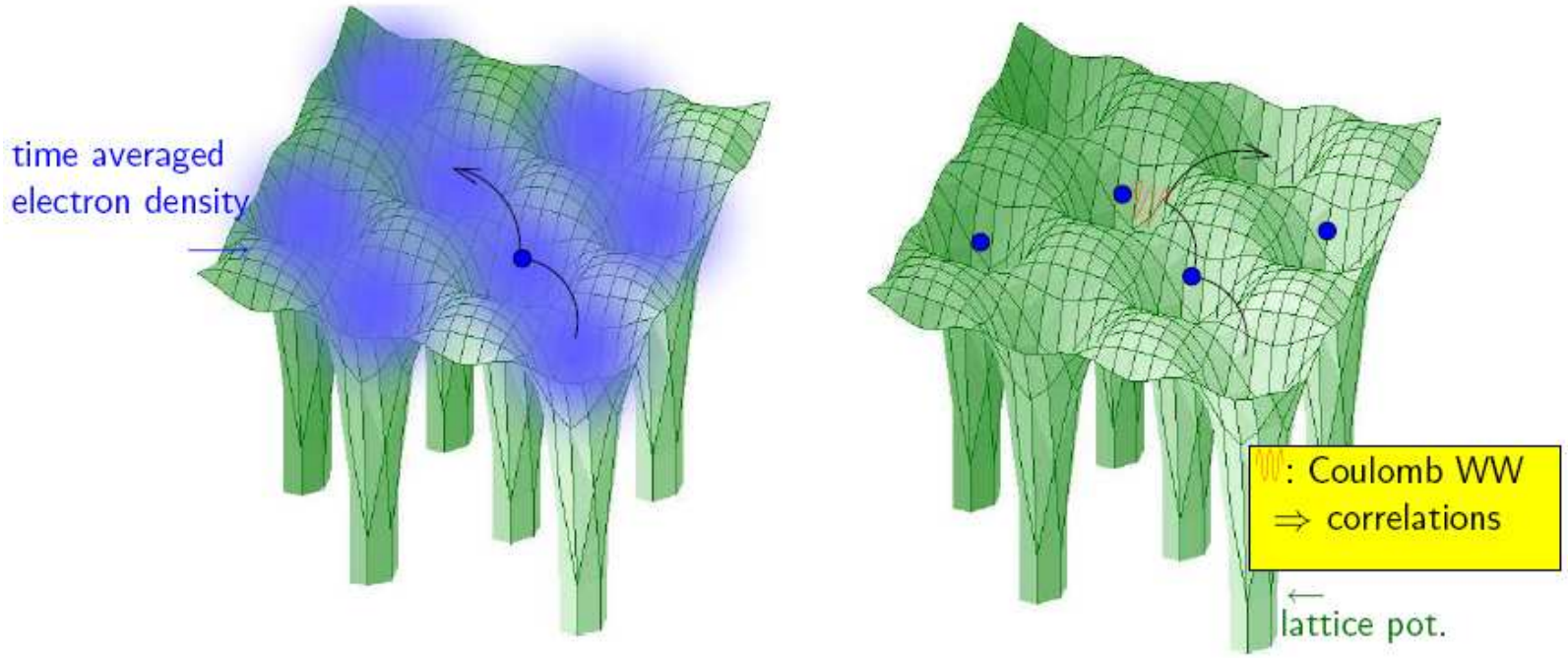


| | | |
|---|---|---|
| **delocalizing effects** | ⇔ | **localizing effects** |
| **kinetic energy: T** | | **Coulomb repulsion: U** |
| **FM metal** | ⇔ | **AFM CO-OO insulator** |

**Tuning between these two phases: chemical substitution (doping), lattice strain, magnetic field, electrical field, . . .**

# Transition Metal Oxides with Perovskite Structure ...

**... display a broad range of interesting phenomena, including ...**

Ideal Perovskite Structure
(Cubic)

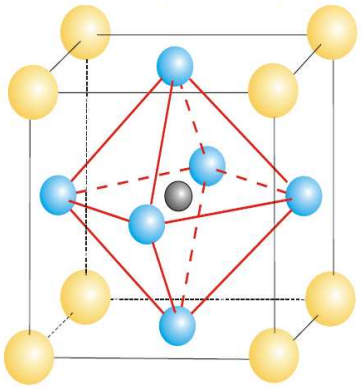

$LaMnO_3$

| | |
|---|---|
| **Electrical** | **High-$T_c$ Superconductivity (HTSC)** |
| | **Cuprates** ( Bednorz & Müller, Nobel Prize 1987 ) |
| **Magnetic** | **Colossal Magnetoresistance (CMR)** |
| | **Manganites** ( → GMR: Fert & Grünberg, Nobel Prize 2007 ) |
| **Electrical & Magnetic** | **Multiferroicity** |

## Manganites: Insulator-Metal Phase Control - $Pr_{0.7}Ca_{0.3}MnO_3$

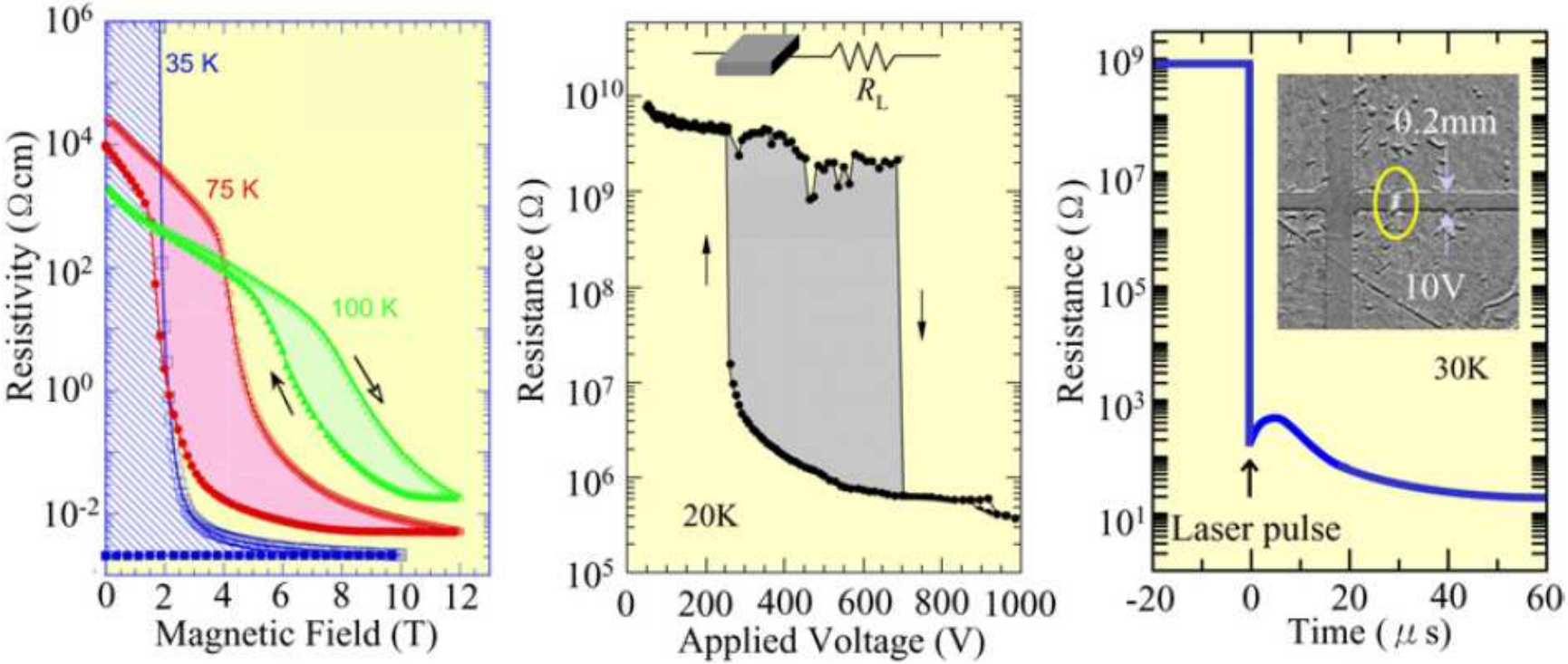


**[Y. Tokura, Rep. Prog. Phys. 69 (2006) 797]**

**MIT control by ”photo doping”: possible on the femtosecond time scale ?**

## High-$T_c$ Superconductivity

# Light-Induced Superconductivity in a Stripe-Ordered Cuprate

D. Fausti,[1,2]*†‡ R. I. Tobey,[2]†§ N. Dean,[1,2] S. Kaiser,[1] A. Dienst,[2] M. C. Hoffmann,[1] S. Pyon,[3] T. Takayama,[3] H. Takagi,[3,4] A. Cavalleri[1,2]*

One of the most intriguing features of some high-temperature cuprate superconductors is the interplay between one-dimensional "striped" spin order and charge order, and superconductivity. We used mid-infrared femtosecond pulses to transform one such stripe-ordered compound, nonsuperconducting $La_{1.675}Eu_{0.2}Sr_{0.125}CuO_4$, into a transient three-dimensional superconductor. The emergence of coherent interlayer transport was evidenced by the prompt appearance of a Josephson plasma resonance in the *c*-axis optical properties. An upper limit for the time scale needed to form the superconducting phase is estimated to be 1 to 2 picoseconds, which is significantly faster than expected. This places stringent new constraints on our understanding of stripe order and its relation to superconductivity.

[ D. Fausti et al., Science 331 (2011) 189. ]

**- this topic will not further be discussed in this lecture -**

# Phase Control in Multiferroics

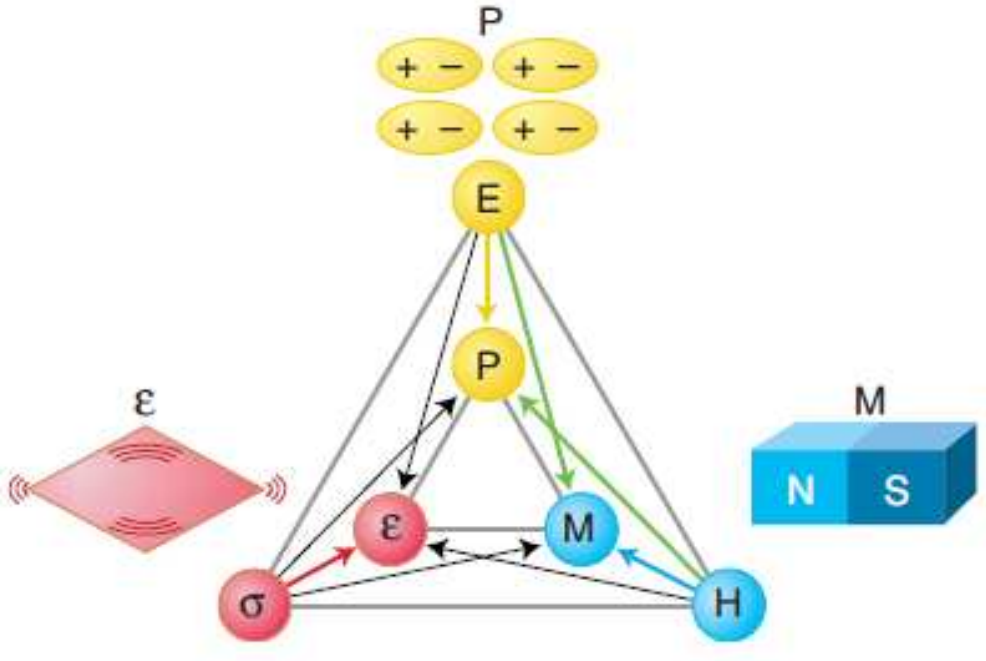


**[ N. Spaldin and M. Fiebig, Science 309 (2005) ]**

**strain $\sigma$ ↔ stress $\epsilon$ / electric field E ↔ polarization P / magnetic field H ↔ magnetization M**

**Magnetoelectric multiferroicity:**
**coexistence of spontaneous ferroelectricity and ferromagnetism**

# Phase Control in Multiferroics

**Thermodynamic expansion of the free energy:**

Landau theory framework, approached by the expansion of free energy for a magnetoelectric system, i.e.

$$F(E,H) = F_0 - P_i^s E_i - M_i^s H_i - \frac{1}{2}\varepsilon_0\varepsilon_{ij}E_iE_j - \frac{1}{2}\mu_0\mu_{ij}H_iH_j - \alpha_{ij}E_iH_j - \frac{1}{2}\beta_{ijk}E_iH_jH_k - \frac{1}{2}\gamma_{ijk}H_iE_jE_k - \cdots, \quad (1)$$

**Derivatives provide polarization P and magnetization M:**

effects parameterized by tensors $\beta$ and $\gamma$ (see [25]). Then the polarization is

$$P_i(E,H) = -\frac{\partial F}{\partial E_i} = P_i^s + \varepsilon_0\varepsilon_{ij}E_j + \alpha_{ij}H_j + \frac{1}{2}\beta_{ijk}H_jH_k + \gamma_{ijk}H_iE_j + \cdots, \quad (2)$$

and the magnetization is

$$M_i(E,H) = -\frac{\partial F}{\partial H_i} = M_i^s + \mu_0\mu_{ij}H_j + \alpha_{ij}E_j + \beta_{ijk}H_jE_i + \frac{1}{2}\gamma_{ijk}E_jE_k + \cdots. \quad (3)$$

**Linear magnetoelectric effect: components $\alpha_{ij}$ of tensor $\alpha$ for P and M** [ M. Fiebig, J. Phys. D: Appl. Phys. 38 (2005) ]

**$\Leftrightarrow$ Recent demonstration of magneto-electric coupling in $TbMnO_3$ (static):** [ H.C. Walker et al., Science 333 (2011) ]

# Motivation

## The essence of Turning Physics into Technology Relies on Control:

**electricity with magnetism**

**magnetism with electricity**

**elasticity with magnetism**

**etc.**

# Multiferroic $ErMn_2O_5$: Manipulating Magnetic Moments with Electric Fields

[Bodenthin PRL 100 (2008)]

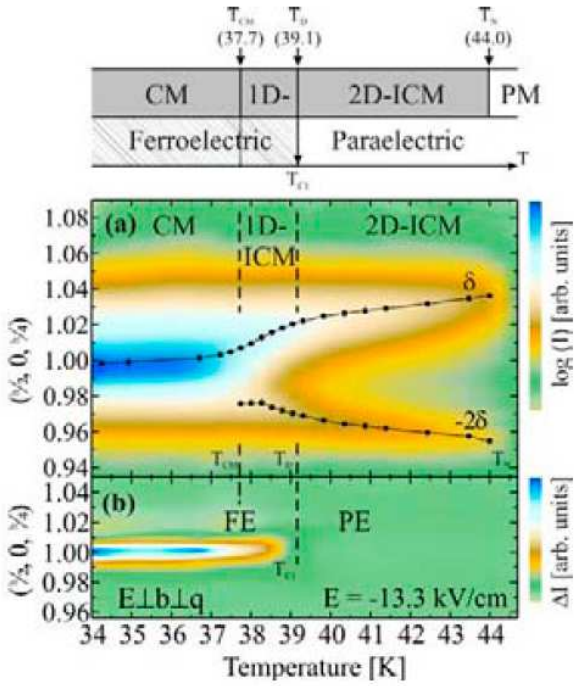


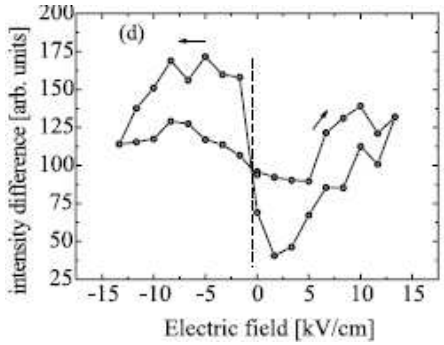


[Cheong & Mostovoy Nat Mat 2007]

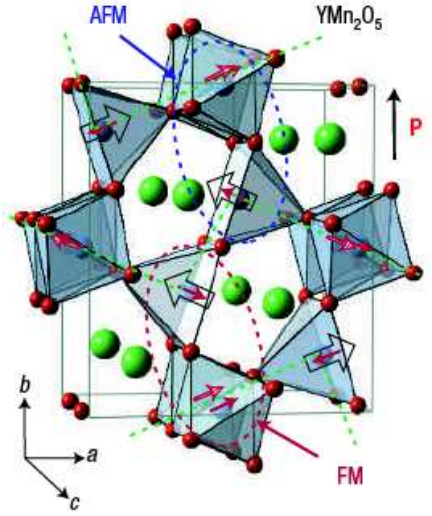


**Spontaneous electric polarization P // b-axis at $T_{C1}$ = 39.1 K induced by non-collinear magnetic moments**

**(a) Static RESOXS on magnetic (1/2 0 1/4) reflection at Mn $L_3$-edge: temperature dependence**

**(b) Intensity difference due to (static) electric field**

**Future plans: use half cycle THz E-fields for ultrafast switching**

# Short remark: stimulated non-equilibrium phase transtition

# Non-equilibrium phase transitions

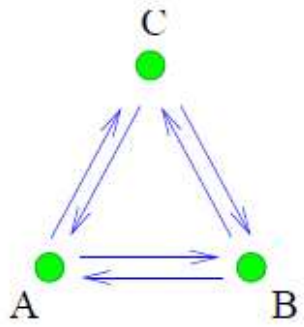


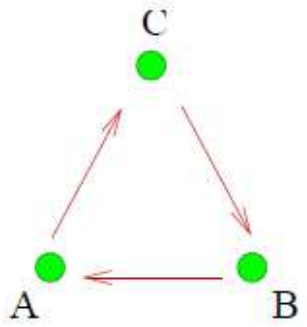


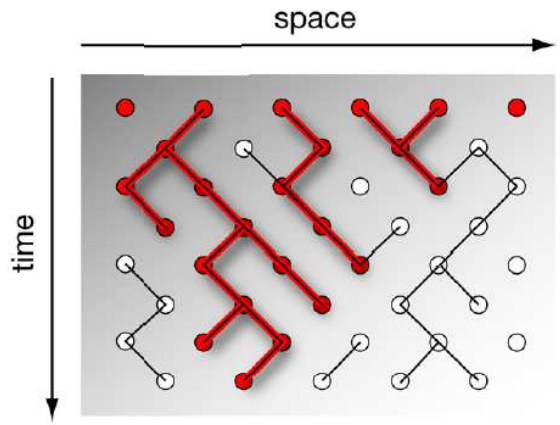


**Thermal equilibrium:**

**Idealized state where all the memory about the initial state is lost due to relaxation processes**

**Microstates A, B, C: Dynamics obeys detailed balance**

⇳

**Nonequilibrium:**

**Dynamic, involving flow of time, on equal footing with spatial coordinates**

**Microstates A, B, C: transitions occur only clockwise, stationary state out of equilibrium**

**[ H. Hinrichsen, University Würzburg ]**

# Stimulated (Photoinduced) Non-Equilibrium Phase Transitions

**equilibrium** ⇔ **?**

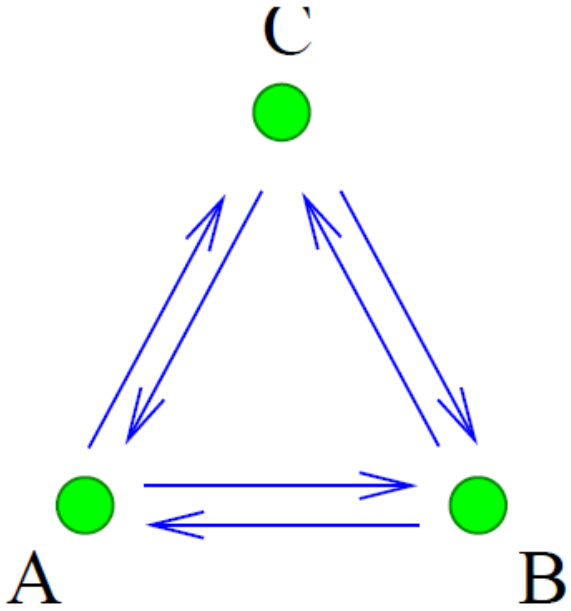


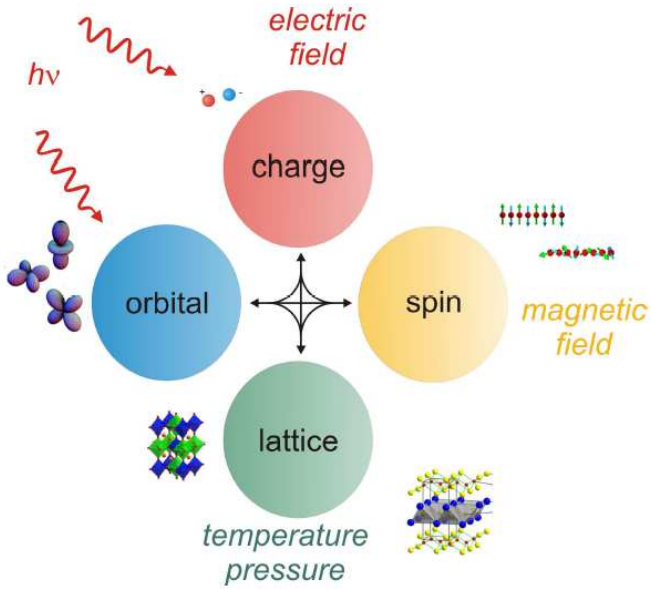


⇕

**Lattice**

**(heat bath)**

## Fingerprint of a nonthermal effect

- **pump - pulse: polarization dependence**
- **double - pump: ultrafast coherent control**

**- We have demonstrated this for coherent phonon excitation (see later) -**

**- Later it has also been shown for coherent spin wave excitation -**

# Double-Pump: Ultrafast Coherent Control of Spin Waves

**IR induced spin waves in $DyFeO_3$**

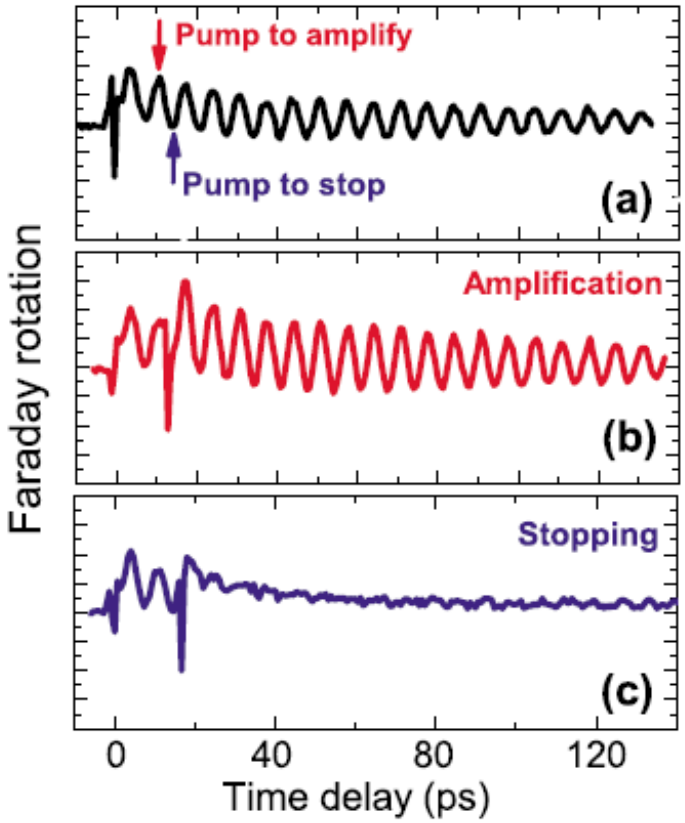


**[ Kirilyuk et al., Rev. Mod. Phys. 82 (2010) ]**

**THz induced spin waves in AFM NiO**

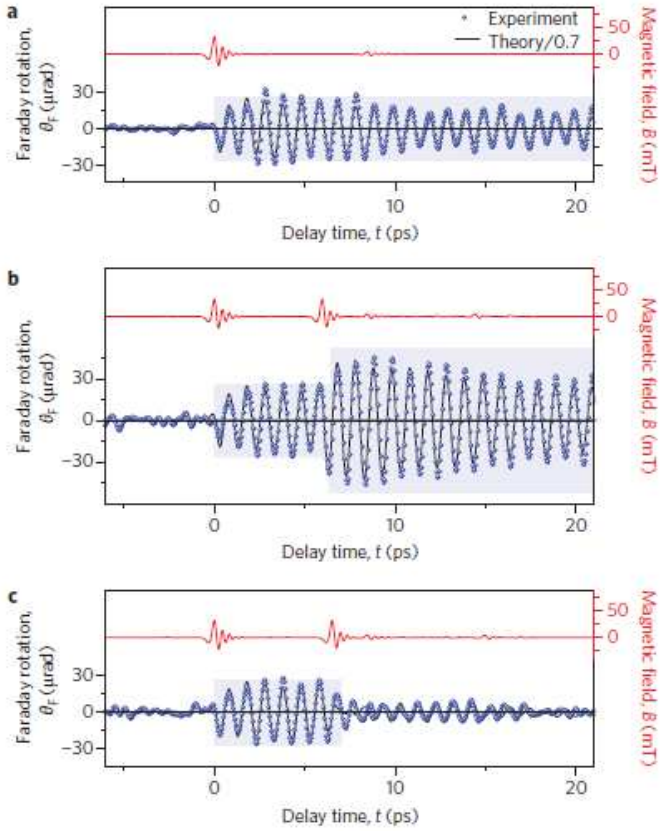


**[ Kampfrath et al., Nat. Photonics 5 (2011) ]**

# pump-probe

**→ all optical: reflectivity & TR-MOKE**

**→ laser-pump / X-ray probe**

## Pump-Probe Measurements

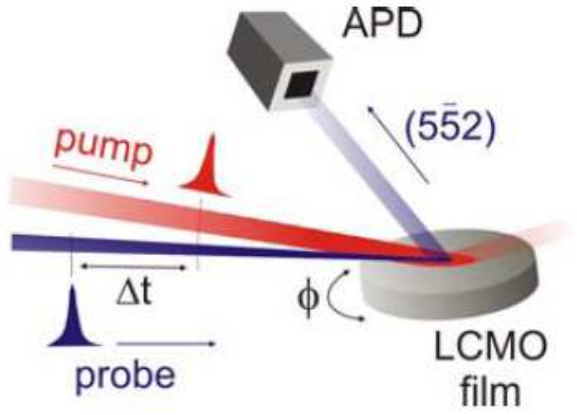


- **pump- or probe-pulse: laser, X-ray, electrons, E-field, H-field, ...**
  **(... choose any combination ... depending on the experiment ... )**

**”Start - Stop” type of experiment**
**( reminds us of time-of-flight measurements, but we don’t use TAC conversion )**

- **trick: convert time-measurement $\Delta$ t $\rightarrow$ distance-measurement $\Delta$ d**
  **( $\leftrightarrow$ use optical delay line: c $\sim$ 0.3 $\mu$m / fs )**

- **pump-probe time delay $\Delta$ t $\rightarrow$ $\Delta$ d = c $\cdot$ $\Delta$ t / 2**
  **( $\Delta$ t = 3 fs $\sim$ $\Delta$ d = 1 $\mu$m )**

# Pump-Probe Measurements

**laser-pump / laser-probe**

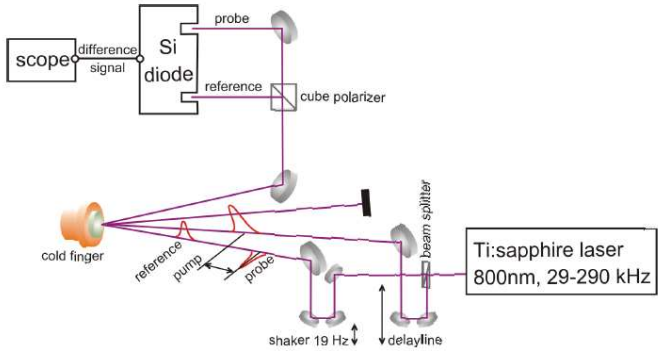


**[ Uni Konstanz ]**

**laser-pump / X-ray probe**

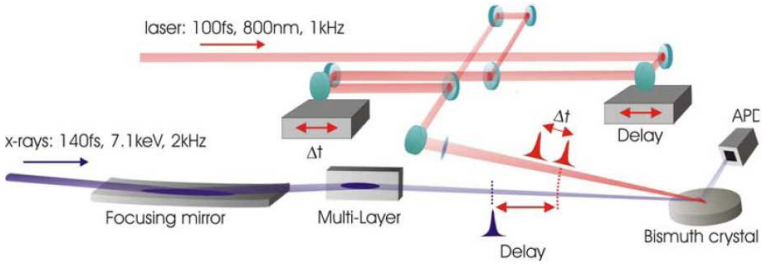


**[ FEMTO / PSI ]**

- **Time-resolved data are recorded as a function of delay time Δ t between pump and probe**

- **Stroboscopic measurement over millions of shots: sample recovery time $\tau_{recov} << 1 / f_{rep-rate}$**

- **Time resolution: $\Delta\tau = \tau_{pump} + \tau_{probe} + \Delta\tau_{syn-jitter} + \Delta\tau_{syn-drift}$**

- **Task: measure pulse lengths $\tau_p$ and the uncertainty $\Delta\tau_s$ due to synchronization jitter and drift**

- **In the IR/optical regime, non-linear effects can be employed**

- **But: cross sections for non-linear effects (i.e. parametric conversion) in the x-ray regime are very small**

**[ P. Eisenberger et. al., PRL 23 (1969); PRL 26 (1971) ]**

# Example 1: All Optical Reflectivity Measurements

## - Coherent Phonons in Charge Density Wave System $TiSe_2$ -

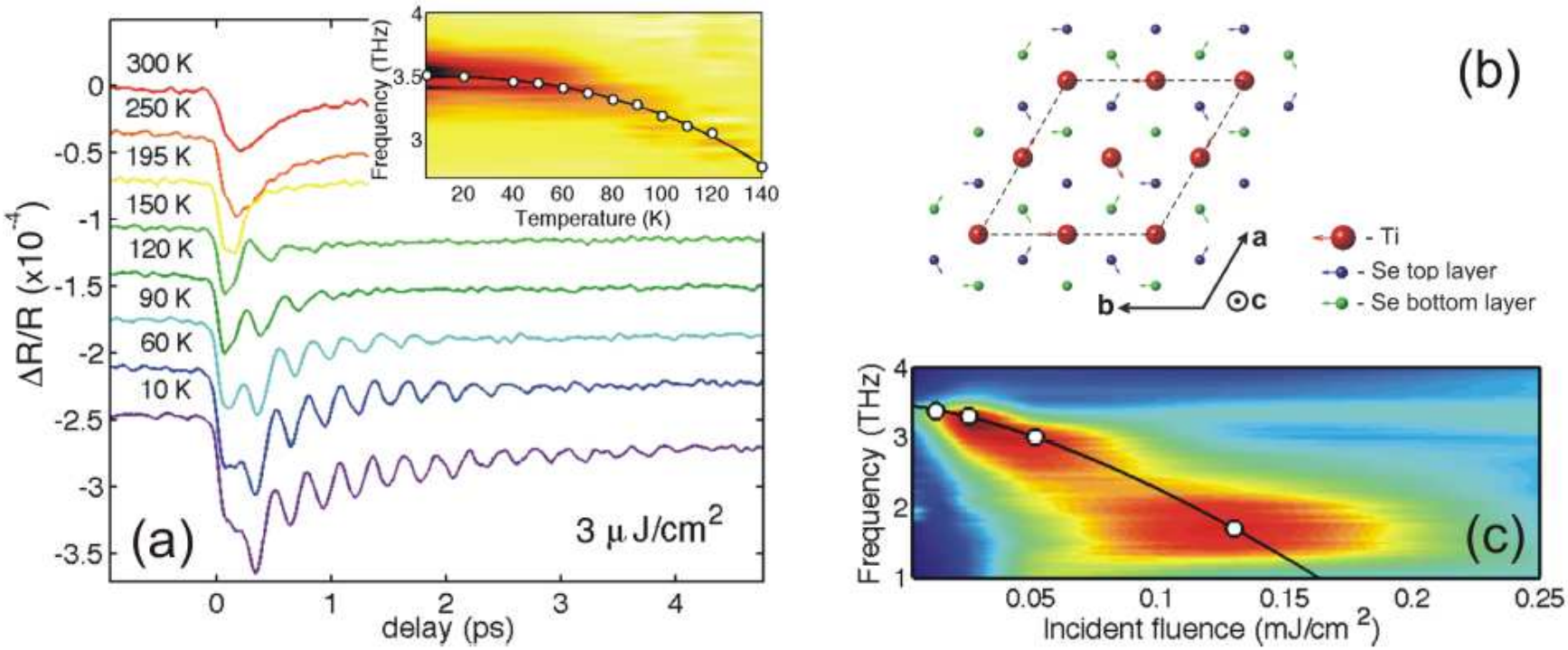


[ Vorobeva et al., Phys. Rev. Lett. 107 (2010) ]

- Optical reflectivity measures the variation of the dielectric function in the material
- Microscopic mechanism ⇒ timeresolved X-ray diffraction (TR-XRD) to track the atomic positions

# Example 2: All Optical MOKE Measurements
## - Demagnetization Dynamics in Ferromagnetic Ni -

**time-resolved magneto optical Kerr measurement (TR-MOKE)**

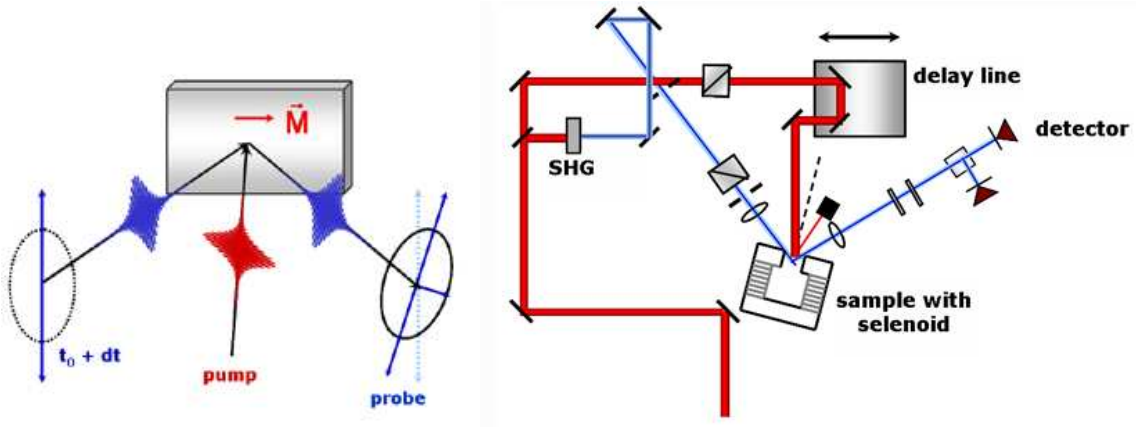


[ http://www.physik.uni-kl.de ]

**magnetization Ni**

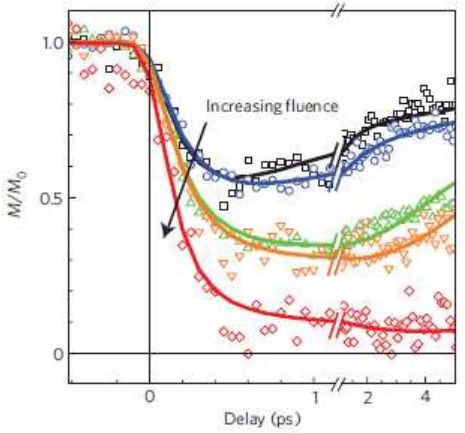


[ Koopmans et al., Nat Mat 9 (2008) ]

- The Kerr rotation and ellipticity depend in first oder linearly on the sample magnetization
- Different transition probabilities of spin-up and spin-down electrons for left & right polarized light

- Microscopic mechanism ⇒ timeresolved resonant X-ray diffraction (TR-RXRD) to track the electronic and spin states in an element specific manner
  ⇒ timeresolved X-ray circular dichroism (TR-XMCD) to track the orbital and spin states separately in an element specific manner

# Example 3: All optical measurement on Phonon-Magnon Coupling
## - Coherent Optical Phonons and Parametrically Coupled Magnons -

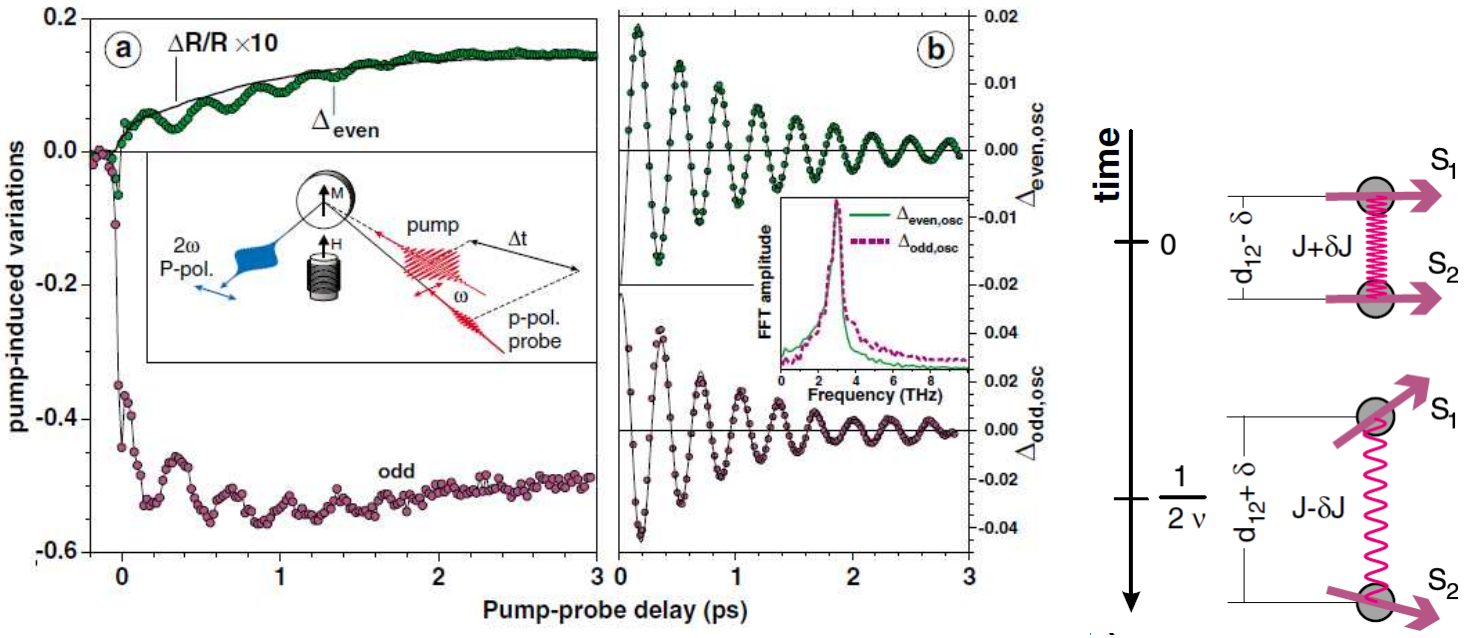


[A. Melnikov et al., PRL 91 (2003)]

- Optical phonons as driving mechanism to coherently excite the spin system in Gd at 3 THz

- Even (odd) reflected SH intensity measures the pump-induced spin (magnetization) dynamics

- Finite transfer time between lattice and spin system below time resolution $\leq$ 100 fs

# Femtosecond X-rays generated with undulators & relativistic e-beams

→ **laser sliced or compressed e-beams**

→ **femtosecond polarized x-rays**

## Femtosecond (fs) X-rays: fs electron bunch $\Rightarrow$ fs X-ray pulse

- Generation of a fs electron pulse: copressing or slicing a long bunch

- Method: manipulation of relativistic electrons in phase space

- Step 1: energy modulation of the e-bunch with oscillating E-field

  compressing: E-field = rf cavity field (correlated energy transfer)
  slicing: E-field = optical laser field (resonant energy transfer)

- Step 2: energy-momentum dispersion in a static B-field

  compressing: B-field $\leftrightarrow$ magnetic compressor
  slicing: B-field $\leftrightarrow$ slicing spectrometer

- Generation of a fs X-ray pulse: undulator radiation

- Step 3: energy-momentum dispersion in a static oscillating B-field

  compressing: XFEL facility $\leftrightarrow$ ampl., coh., lin & circ pol., fs X-rays
  slicing: slicing facility $\leftrightarrow$ spon., incoh., lin & circ pol., fs X-rays

# Femtosecond Slicing Source FEMTO at SLS: 5 - 12 keV

**Resonant laser-electron interaction in a static undulator magnetic field:**

**1. step: modulator** **2. step: dispersion** **3. step: radiator**

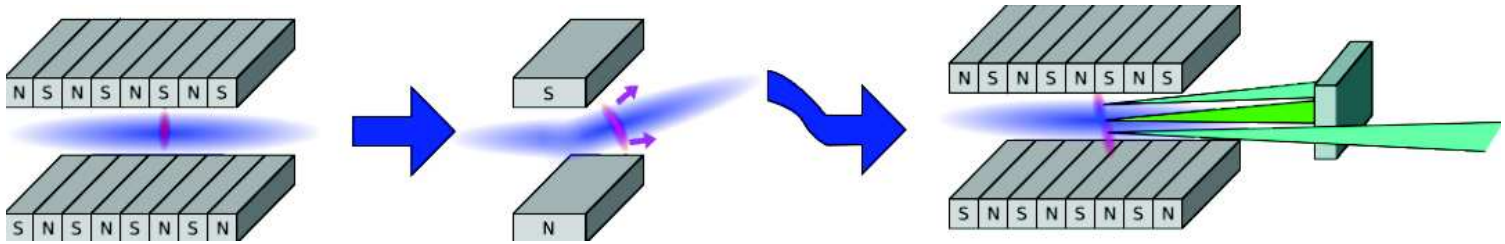


**laser energy modulation** **pulse separation** **fs X-ray generation**

[ R. Schoenlein et al., Science 287 (2000); S. Khan et al., PRL 97 (2006); P. Beaud et al., PRL 99 (2007) ]

- Only the laser electric field ($\sim 10^{10}$ V/m) couples to the electrons
- Highly relativistic electrons: laser magnetic field ($\sim 30$ T) does not affect the electron trajectory

# Femtosecond Soft X-Rays & Flexlibe Polarization: 0.5 - 2.5 keV

**BESSY slicing facility**

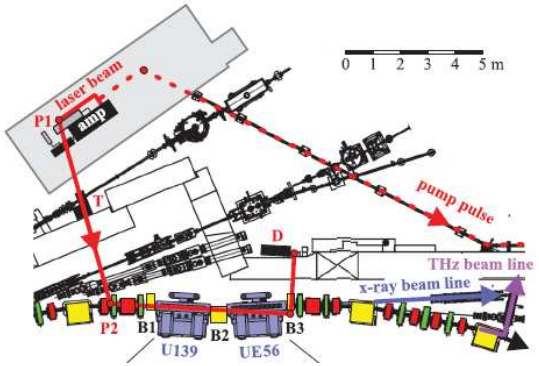


**[ S. Khan et al., PRL 97 (2006) ]**

**APPLE II undulators: lin / circ pol**

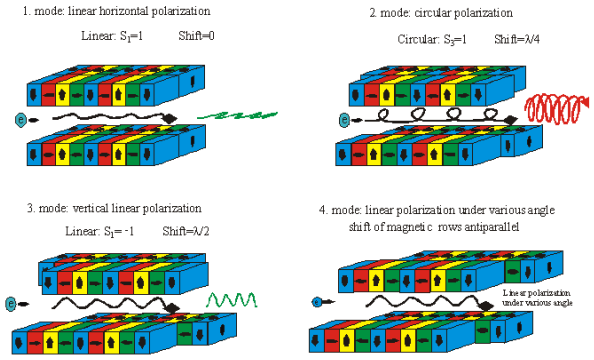


**[ J. Bahrdt et al., NIM A 467 (2001) ]**

**measured Stokes parameters**

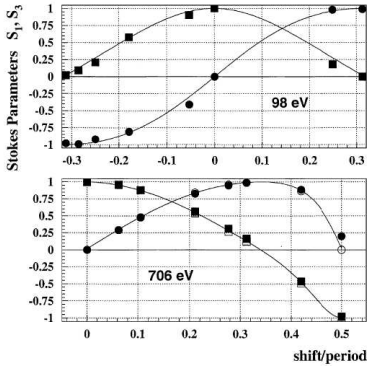


**Example TR-XMCD: fs demagnetization in ferromagnetic Ni - spin & orbital momentum dynamics**

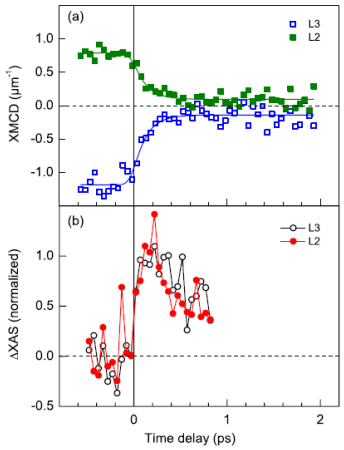


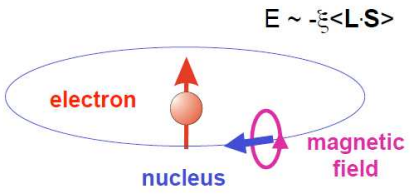


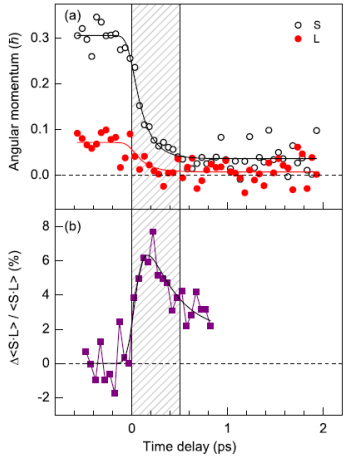


**[ Ch. Stamm et al., Nat Mat 6 (2007); Phys. Rev. B 81 (2010); I. Radu et al., Nature 472 (2011) ]**

# FEMTO Slicing Source: Laser-Pump/X-Ray-Probe Experiments (200 fs)

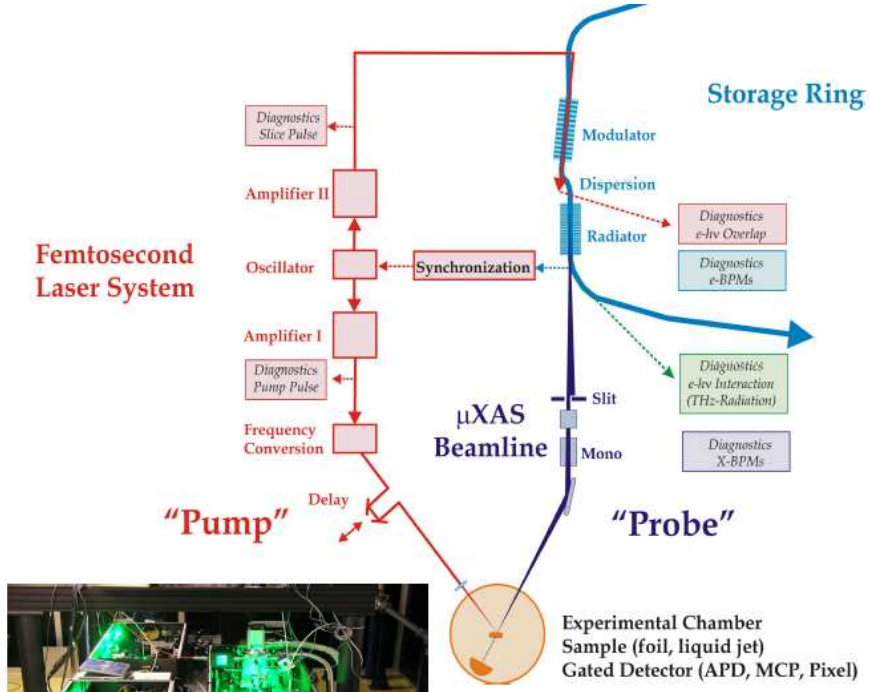


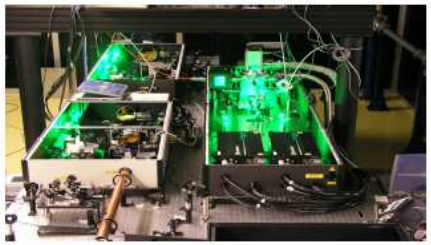

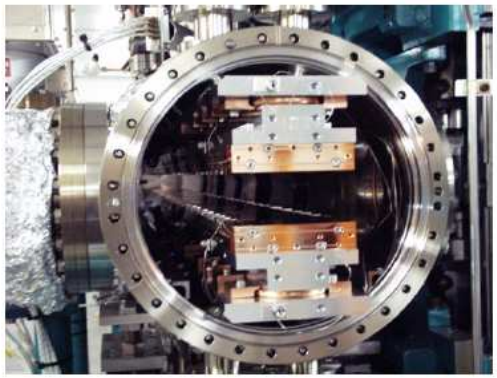

**Laser-synchronization: cavity feedback**

**Electron orbit: position feedback & top operation**

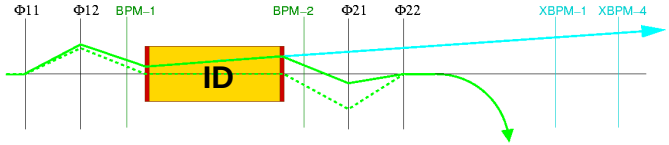


**Feedback systems ⇔ Spatiotemporal stability** [G. Ingold, AIP Conf. Proc. 879 (2007)]

# Pump-Probe Experiments - Laser Slicing Source - Synchronization

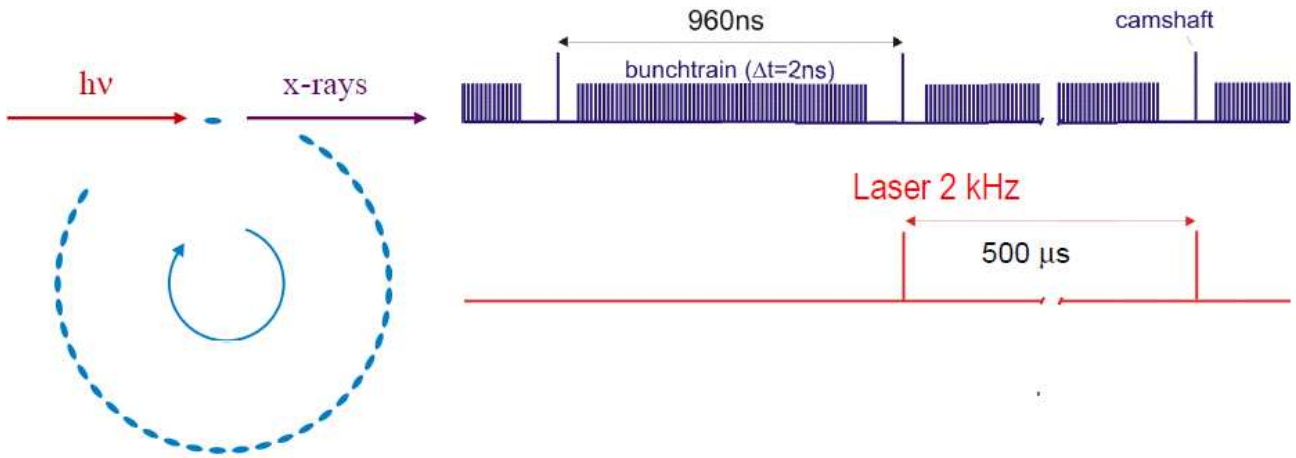


- Laser oscillator (100 MHz) synchronized to 500 MHz RF clock (<<1ps)
- Electron bunches ~ 90 ps
- Slicing Laser: $\tau$ = 50 fs, 2 kHz
- Pump laser: $\tau$ = 100 fs, 1 kHz (seeded from same oscillator)
- Gated detectors: APD's, gated strip or pixel detector (single photon counting)
- Probe alternately „pumped" and „unpumped" sample

# FEMTO Slicing Source: Laser-Pump /X-Ray-Probe Experiments

## - Inherent Synchronization -

**fs-laser system:** oscillator → Amplifier-I (pump)
→ Amplifier-II (slicing/probe)

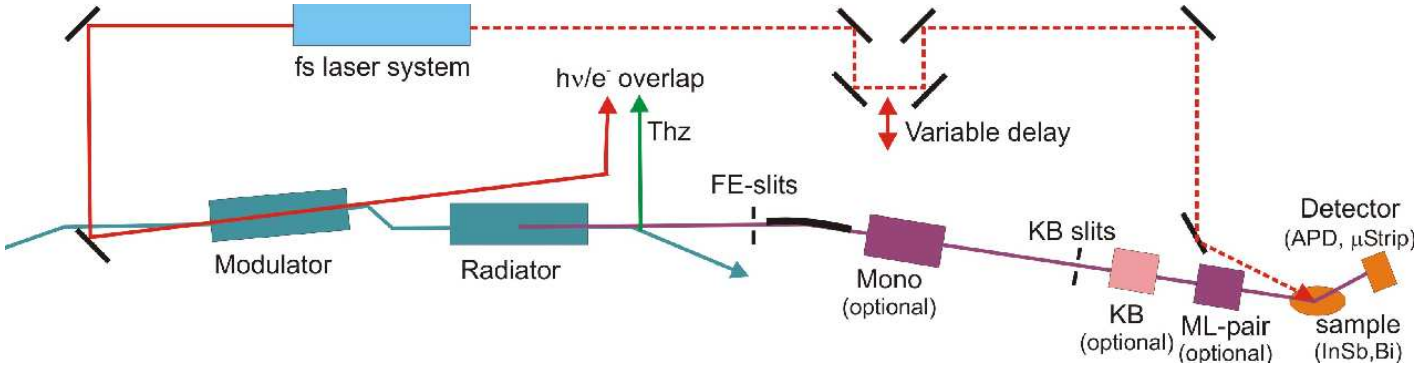


**Slicing spectrometer:** modulator - dispersion - refocussing - radiator

**Beamline:** mirror - mono (Si 111) - KB-optics (refocussing) - mono (multilayer ML)

**Diagnostics:** laser/e-beam timing & overlap (CSR)

**Detectors (gated):** APD, [⇒ $\mu$Strip-, Pixel-detector (PSI detector group)]

**Measured sliced flux:** $4 \cdot 10^5$ ($2 \cdot 10^5$) ph/s/0.1% bw at 5 (8) keV (rep rate 2 kHz)

**Upgrade (proposed):** x 20 flux increase

# Bismuth: Peierls System - Coherent Phonon excitation

**Bi unit cell**

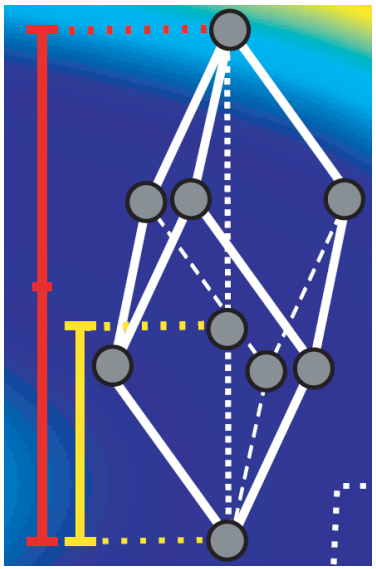

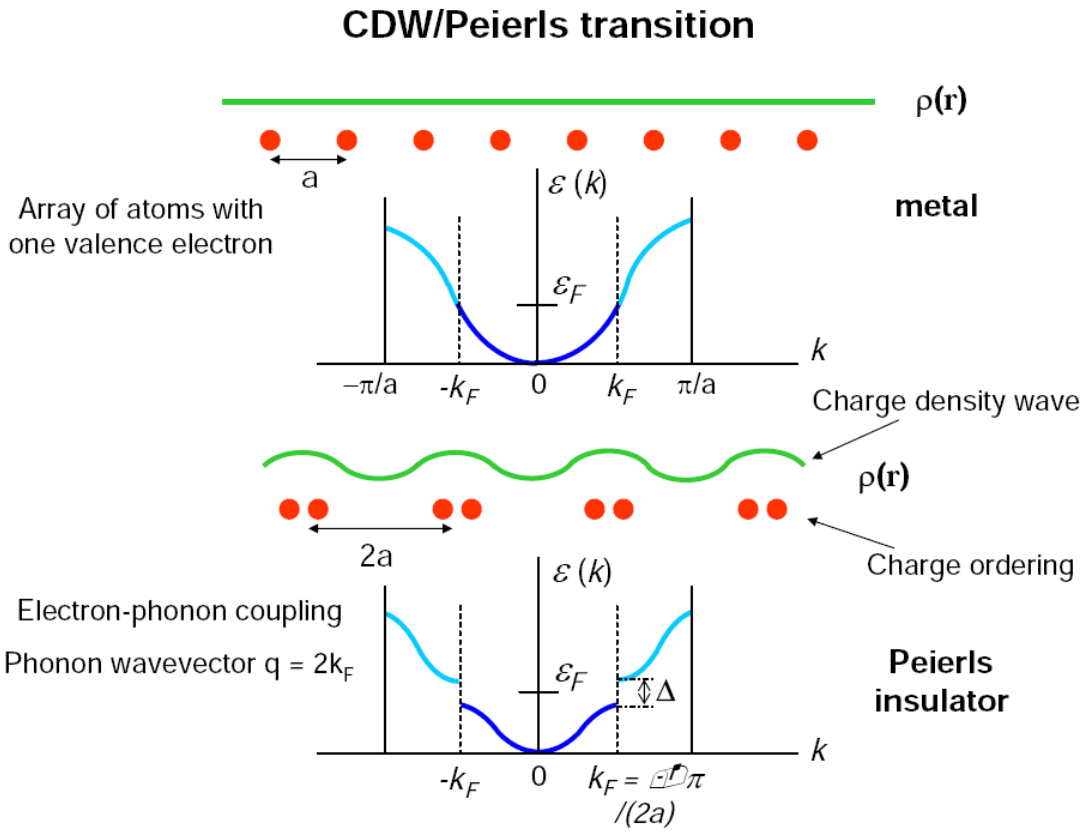


**possible mechanism for charge denstiy wave (CDW) formation (see slide 30)**

# FEMTO: Sub-ps Pulse Length Measurement of Electrons and X-Rays

**Electrons: Interferometry**

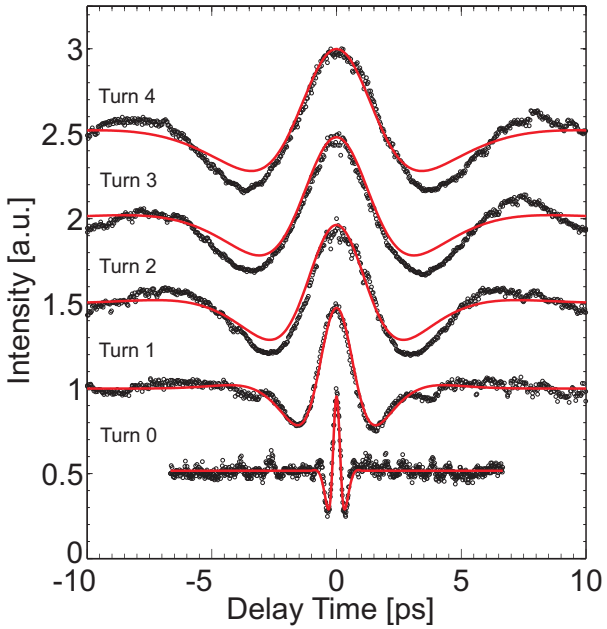


**X-Rays: Optical Phonon Oscillations**

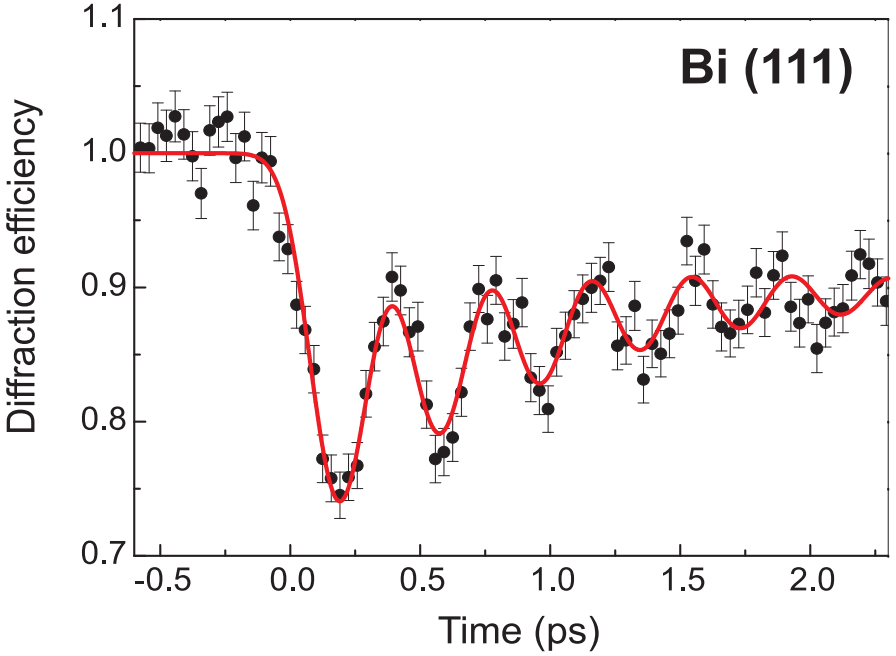


**Electrons: autocorrelation spectra $\sim$ 200 fs FWHM (assuming Gaussian sliced bunches)**

**X-rays (7.1 keV; laser fluence: 2 mJ/cm$^2$):**

**Oscillation frequency:** 2.60 $\pm$ 0.05 THz

**Fitted x-ray pulse width:** 140 $\pm$ 30 fs [FWHM]

**Time resolution $\Delta\tau$:** 195 $\pm$ 25 fs [FWHM]

# Grazing Incidence TR-XRD & 2-Pulse Excitation ↔ Spatiotemporal Stability

**spatial stability**

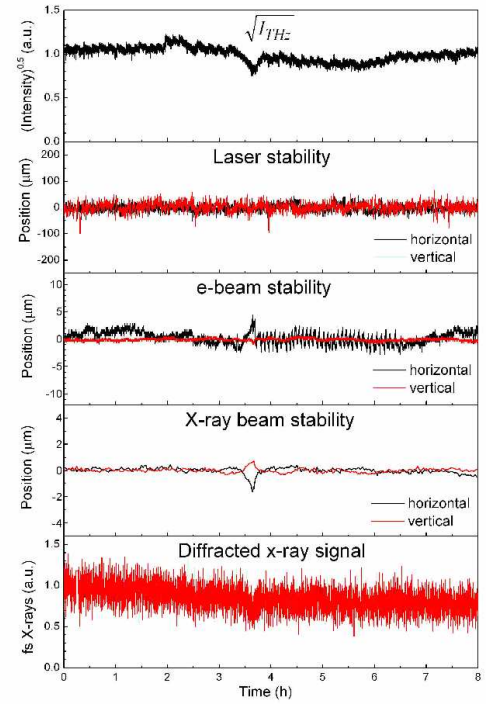


**coherent control: phonon**

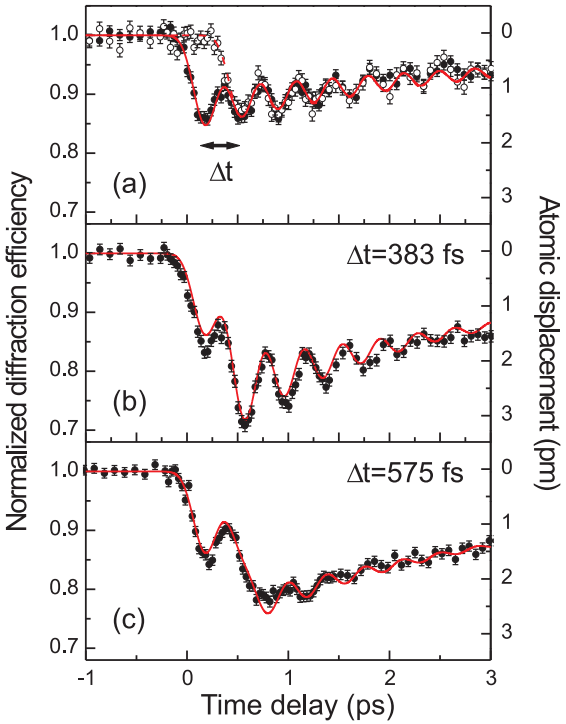


**timing jitter & drift**

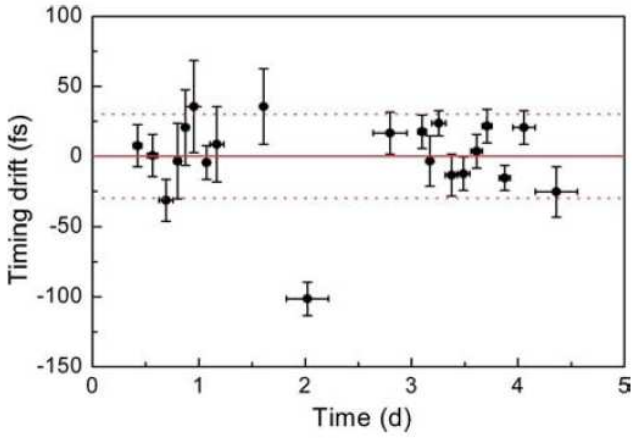


[ P. Beaud et al., PRL 99 (2007) & PRL 100 (2008) ]

- **Double pulse excitation: coherent control of $A_{1g}$ optical phonon in Bi at 2.6 THz.**
- **Temporal stabiliy $\Delta\tau_{syn-jitter} + \Delta\tau_{syn-drift}$: 30 fs (rms) ⇔ spatial stability on sample: $\leq 5\ \mu$m**
- **Longterm temporal stability for hours (days) allows data accumulation over millions of shots.**

# Femtosecond X-Ray Diffraction: Mapping the Int eratomic Potential

## - Laser/X-Ray Pump-Probe: Comparison of Different Timing Methods -

**SPPS/Linac: Arrival Time Stamping**

**pulse compression**

**28 Gev, data acquisition: 0.3 h**

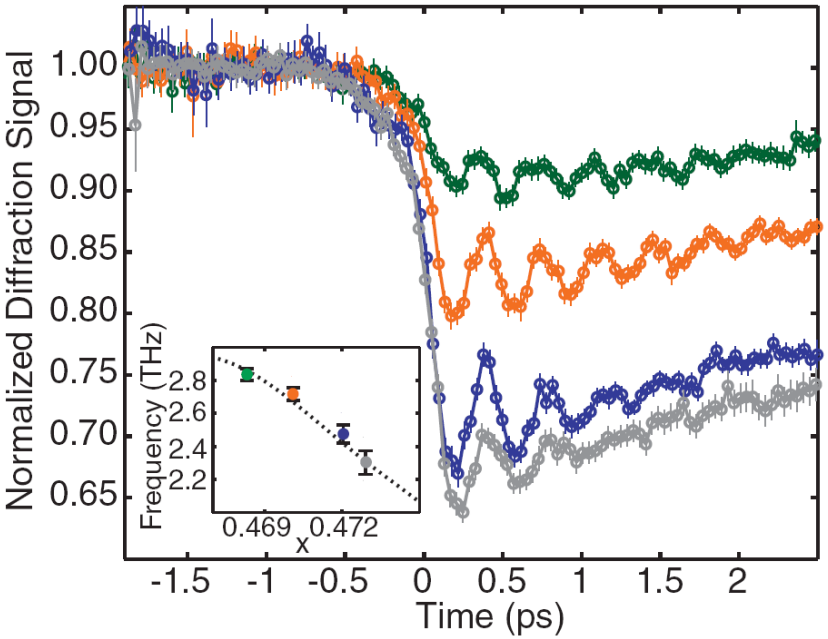


[D.M. Fritz et al., Science 315 (2007)]

**FEMTO/SLS: Inherent Synchronization**

**pulse slicing**

**2.4 GeV, data acquisition: 2-4 h**

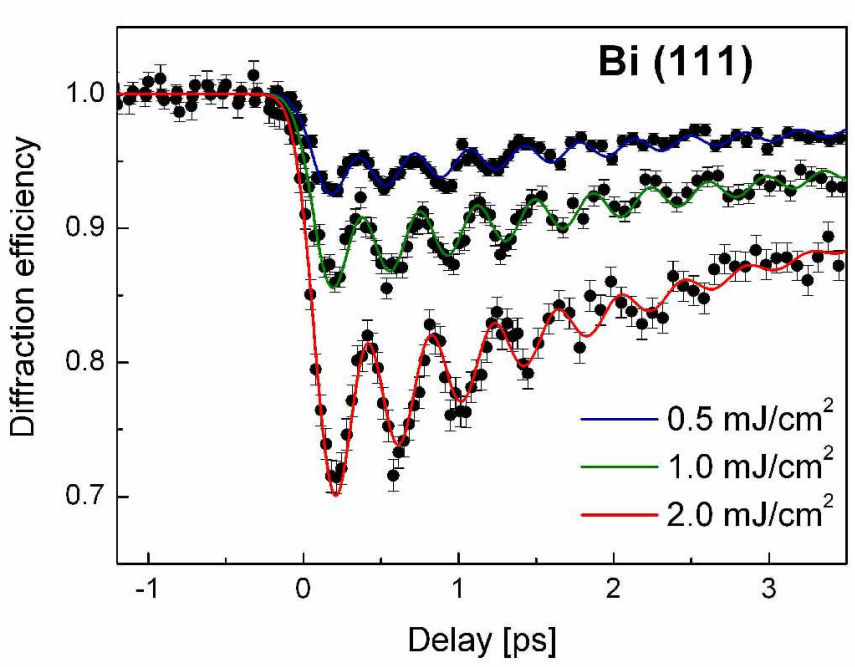


[S. Johnson et al., PRL 100 (2008)]

**Arrival time of electron bunches measured with EO-sampling** [A.L. Cavalieri et al., PRL 94, (2005)]

# SwissFEL (proposed): hard & soft X-ray FEL

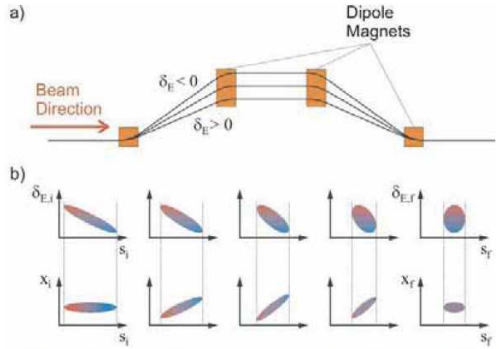


Fig. 1.2.3: The rotation of electrons in the energy–time plane by a magnetic chicane. $\delta_{E,i}$ represents the relative energy spread over the bunch, $s_i$ is the longitudinal coordinate along the bunch and $X_i$ is the transverse beam size (Figure Courtesy of A. Bolzmann [7]).

- SASE XFELs: several are operating or under construction
- SACLA/Spring-8: most compact hard X-ray facility worldwide
- Slicing facility → XFEL-facility: 3 major advantages

  (1) average flux [ph/s]: x $10^6$ - $10^7$

  (2) pulse length [fs]: 100 → 1 - 10

  (3) coherence: trans & long (seeding)

SwissFEL: soft & hard X-ryas

- Challenge at SASE XFEL: Laser-pump / X-probe
- Time resolution $\Delta\tau \leq 10$ fs
- SASE is operated as single pass

  ⇒ X-ray arrival time has been measured

  ⇒ Single shot resolution needed: few fs !
- Promising approach: photoemission IR / THz streaking

  [ F. Tavella et al., Nat Photonics 5 (2011) ]

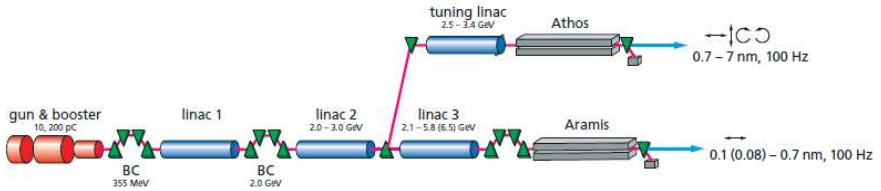


[ http://www.psi.ch/swissfel ]

# Femtosecond grazing incidence X-ray diffraction

→ **experimental setup**

→ **phonon dynamics in semimetals**

→ **phonon-phonon coupling**

→ **hot carrier & phonon dynamics**

# Laser-pump / X-ray-probe experimental station

## Pump-probe setup (2-pulse excitation)

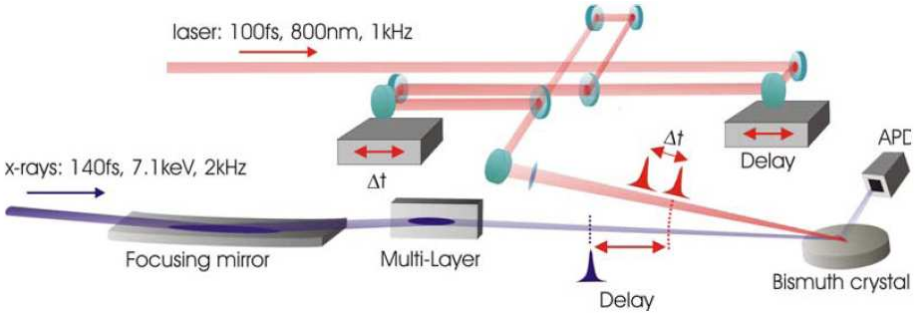


## Pixel detector (gateble)

## (PSI Detector Group)


Pilatus pixel detector

- 487 x 195 pixels = 94965 pixels
- Active Area 83.8 x 33.6 mm²
- Pixel size: 0.172x0.172 mm²
- Dynamic range/pixel: 20bits
- Readout time: 4 ms
  - Longer than FEMTO bunch period

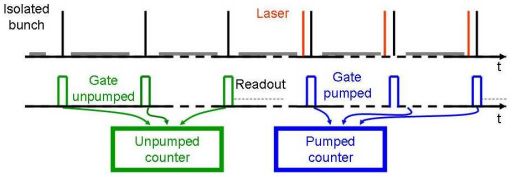


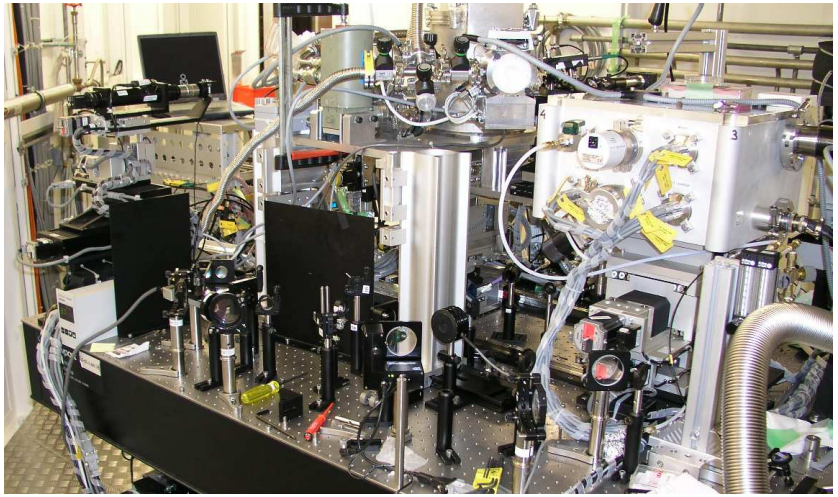

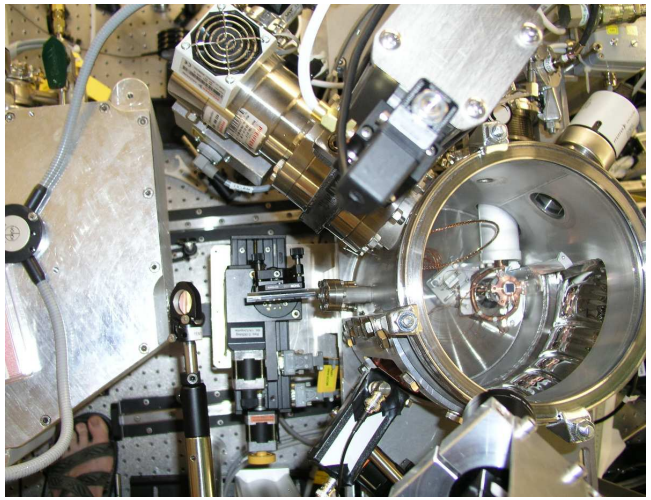

# Grazing Incidence X-Ray Diffraction

**asymmetric cut crystal**

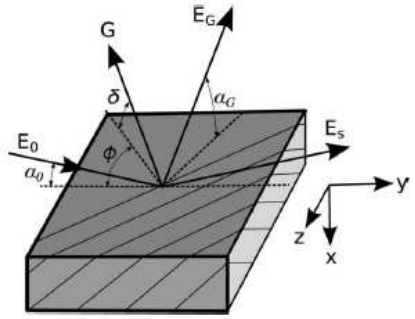


**Figure 2**
Schematic of the X-ray diffraction geometry for non-coplanar grazing incidence from lattice planes with reciprocal-lattice vector **G**. The incident beam ($\mathbf{E}_0$) enters the sample at a glancing angle $\alpha_0$, and two beams leave the surface: a specular reflected beam ($\mathbf{E}_s$) and a diffracted beam ($\mathbf{E}_G$).

**Bi: normalized diffraction from (ijk) planes**

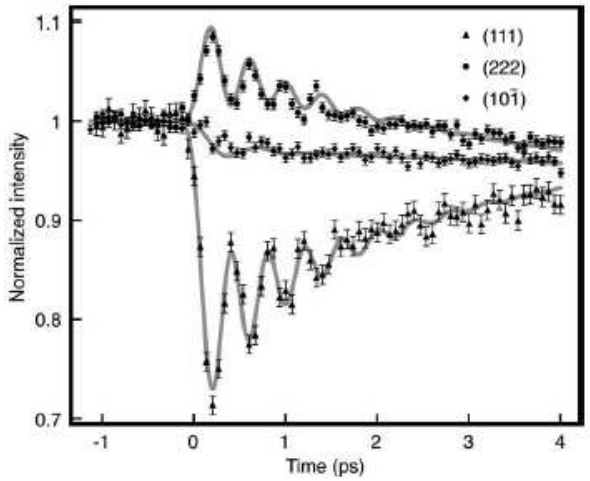


[ S.L. Johnson et al., Acta Cryst. A66 (2010)]

**Diffracted intensity: $I \sim |F|^2$, structure factor: $F = \sum_j f_j e^{-iG\cdot r_j} e^{-W_j}$**

**($f_j$: scatt. form factor, G: recipr. lattice vector, $r_j$: atom lattice position, $e^{-W_j}$: Debye-Waller factor)**

**$\Rightarrow$ Homogenous (optical) phonon excitations: modify structure factor within the unit cell**

**$\Rightarrow$ Measure time-dependent diffraction efficiency as a function of sample rotation angle $\phi$**

# Grazing incidence: matching of pump- and probe volume

- Laser absorption length in opaque media is typically ~10–100 nm, but x-rays probe much deeper
- Grazing incidence diffraction geometry:
  - incidence angle defines probe depth
  - can be applied to crystals
  - grazing incidence → broad rocking curves → multilayer → higher flux
  - efficient absorption of laser at ~10° incidence

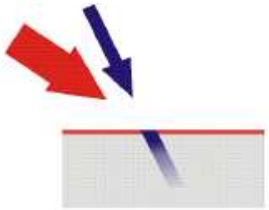

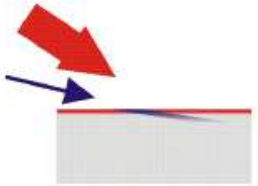

**Bi: depth profile (7 keV)**

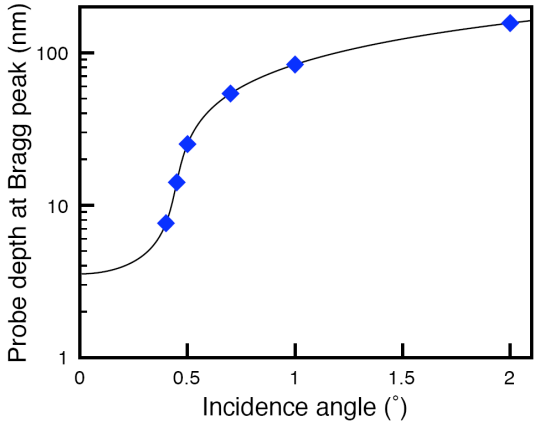


- X-ray absorption length $L_{abs}$ depends only on the wavelength and the incident angle

# Mechanisms of Coherent Phonon Excitation

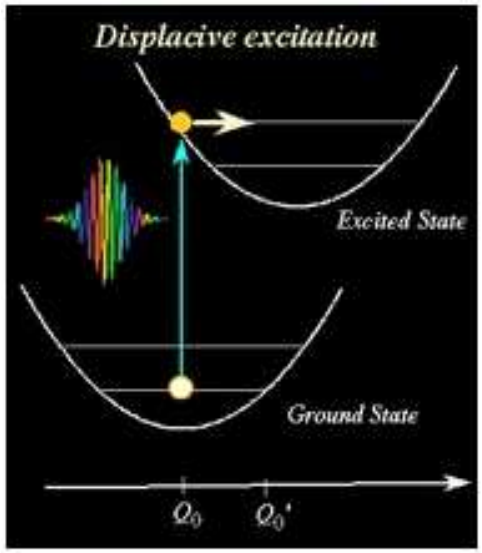


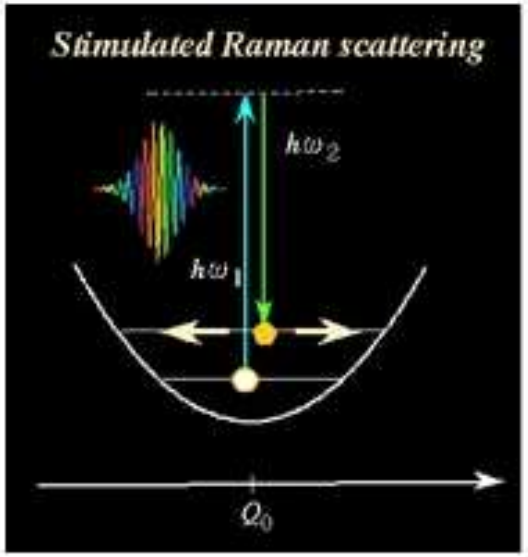


[ figures: K. Ishioka, NIMS, Japan ]

**Phonon amplitude at $t_0$:** **at maximum** **at minimum**

**Time dependence:** **cos-function** **sin-function**

**- Displacive excitation:** **excited carriers push the atomic potential V(z) much faster than the vibrational period that forces the atoms to oscillate around the new minimum of V(z).**

**- Raman scattering:** **inelastic photon scattering via an intermediate vibrational state having a virtual energy level; the process must involve the polarizability of the material.**

# Application 1: Bismuth - Search for $A_g$-$E_g$ Phonon-Phonon Coupling

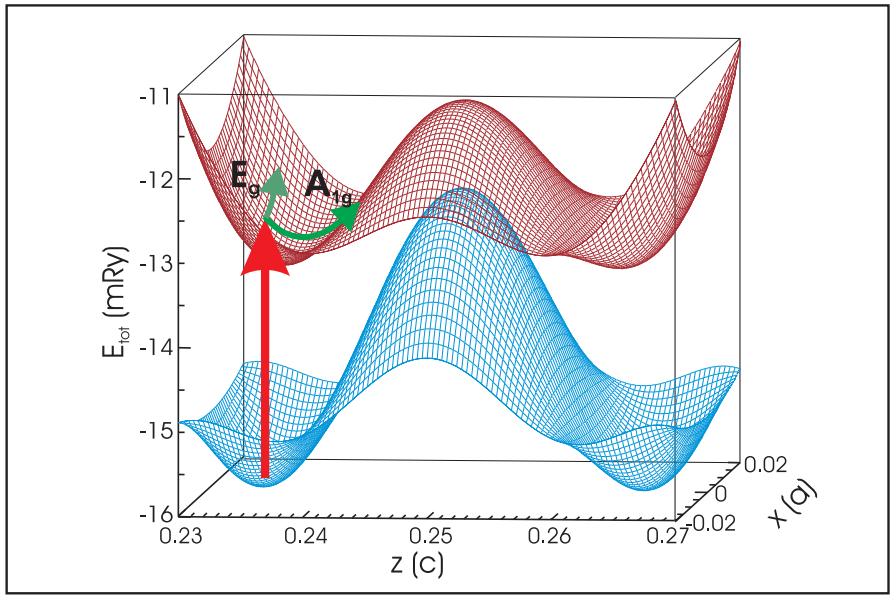


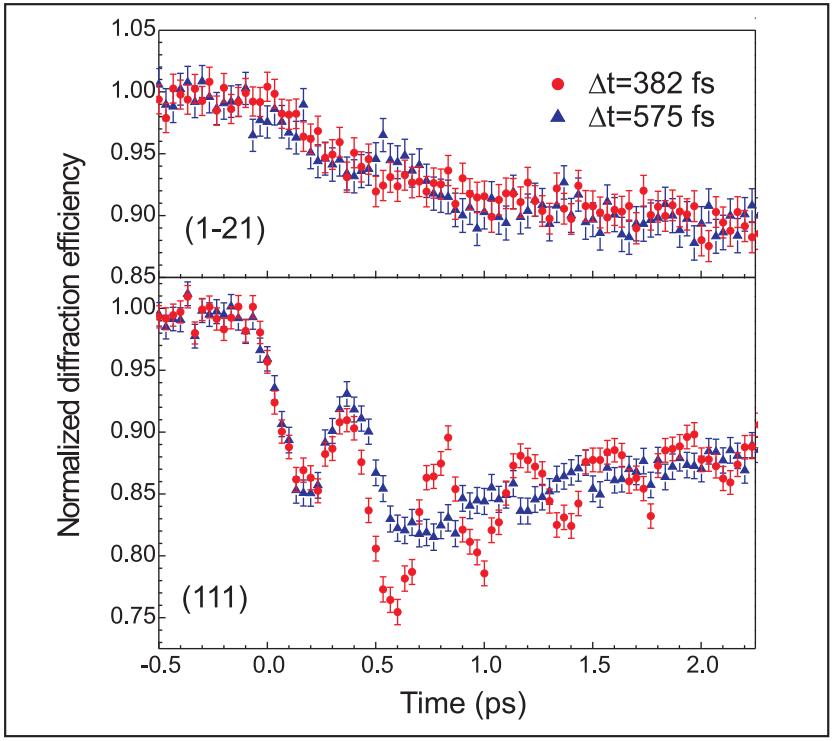


- Potential energy surface for Bi: $A_g$ & $E_g$ mode coupling predicted by DFT theory

- No change of $E_g$ (1-21) diffraction signal by coherent control of $A_g$ (111) motion (double pulse excitation)

# Application 2: $E_g$ Mode in Bi - Direct Observation via Polarization Control

Preliminary results, to be published, S. L. Johnson *et al*.

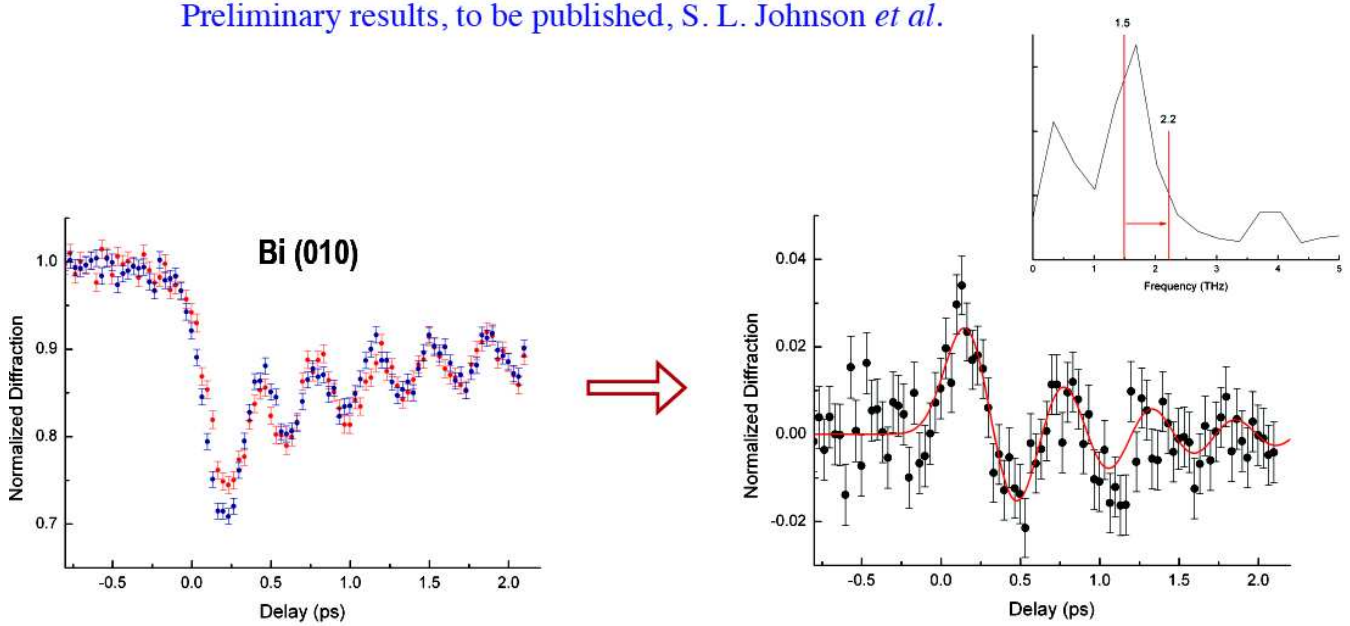


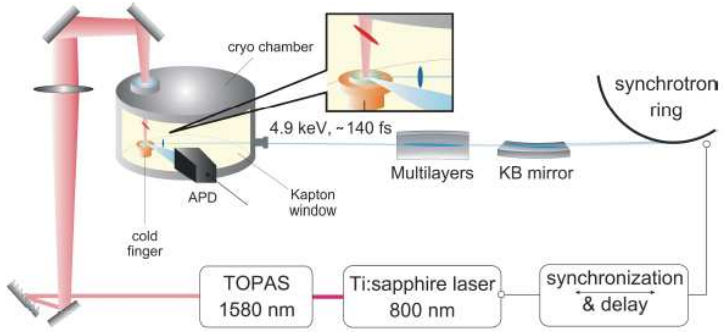


**Laser wavefront tilting allows excitation with two polarizations rotated by 90° (at 170 K)**

# Application 3: fs XRD - Nanoscale Depth-Resolved Lattice Dynamics in Bi

**$A_{1g}$ optical phonon**

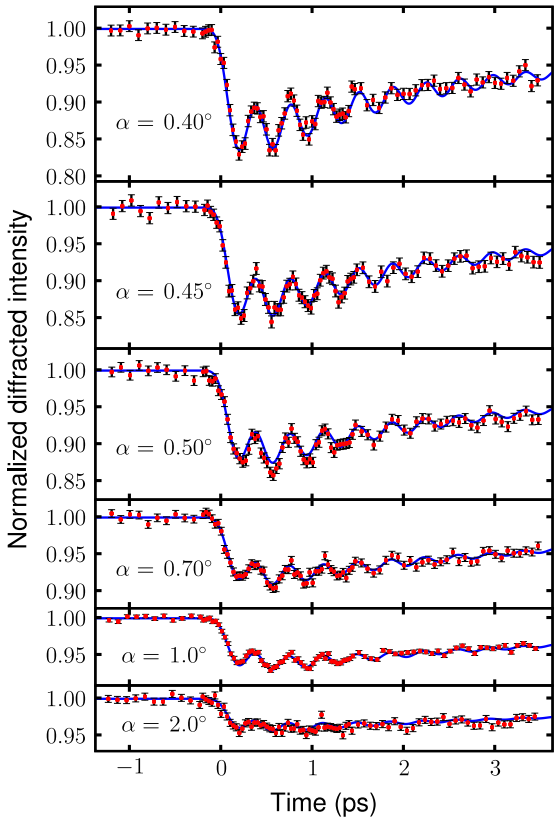


**$z_{eq}$ = 0.2334 ( in units c = 1.18 nm)**

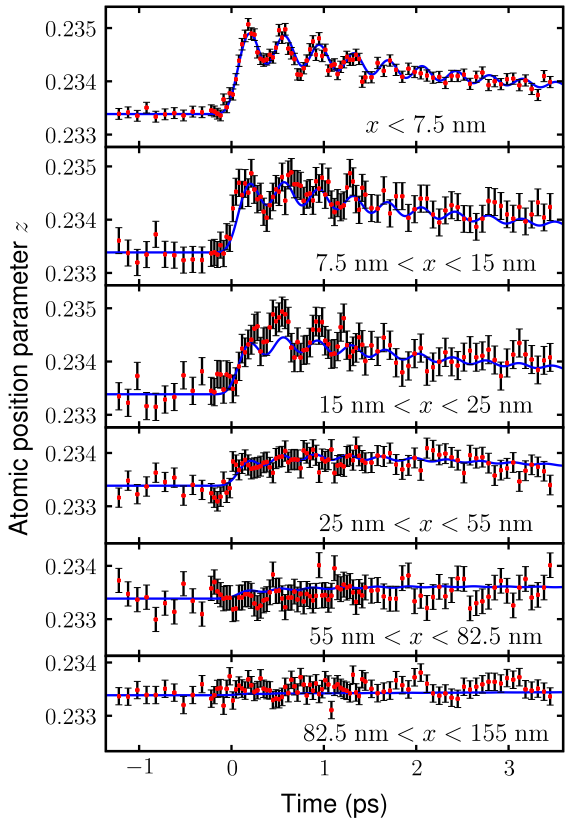


[S.L. Johnson et al., PRL 100 (2008)]

**- information on hot carrier dynamics: timescales of e - h, e - ph interactions & carrier diffusion**

**- nm depth resolution required to separate effects**

# Application 3: fs XRD - Nanoscale Depth-Resolved Lattice Dynamics in Bi

**Grazing incidence angle: $0.5^0$**

| Quantity | Fit | DFT |
|---|---|---|
| Electronic interaction time | $260 \pm 20$ fs | - |
| Diffusion constant | $2.3 \pm 0.3\,\mathrm{cm}^2/\mathrm{s}$ | - |
| Thermalization factor f | $0.53 \pm 0.06$ | 0.42 |
| Softening factor $\beta$ | $248 \pm 7$ THz | 230 THz |
| Amplitude factor $a_1$ | $(0.51 \pm 0.05) \times 10^{-5}\,\mathrm{cm}^3/\mathrm{J}$ | $0.77 \times 10^{-5}\,\mathrm{cm}^3/\mathrm{J}$ |
| Phonon damping rate | $1.01 \pm 0.11\,\mathrm{ps}^{-1}$ | - |
| Electronic relaxation time | $7.6 \pm 0.6$ ps | - |
| Time resolution | $193 \pm 8$ fs | - |

- Time scale for thermal equilibration of the carriers with the lattice: $\tau_1$ = 7.6 $\pm$ 0.6 ps
- Time scale for thermal equilibration between electrons and holes: $\tau_2$ = 260 $\pm$ 20 fs
- Coherent phonon damping rate: $\gamma$ = 1.01 $\pm$ 0.11 $\mathrm{ps}^{-1}$
- X-ray absorption length: $L_0$ = 26 $\pm$ 2 nm

# Related Topic: Hot Carrier & Phonon Dynamics in Solar Cell Materials

**Increase efficiency 31% (Si) → > 66% ? Problem: hot electrons are lost as heat (→ phonons)**

**⇔ transfer demonstrated in PbSe nanocrystals (pump-probe at 810 nm)** [ W.S. Tisdale et al., Science 328 (2010) ]

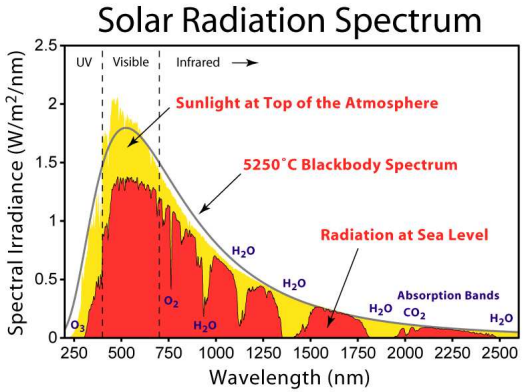


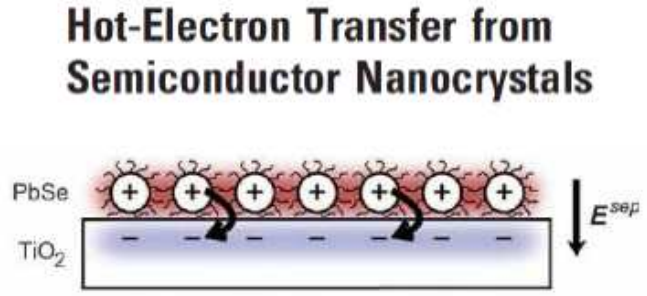


**competition e-transfer ↔ relaxation**

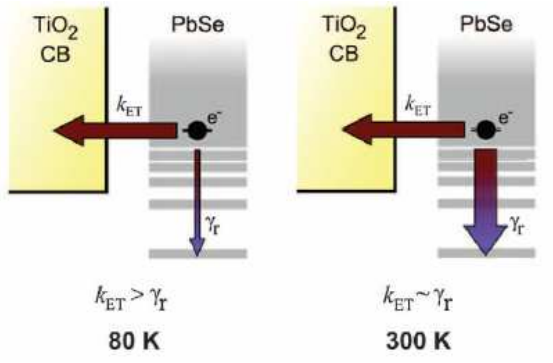


**peak: e-transfer < 500 fs / tail: relaxation**

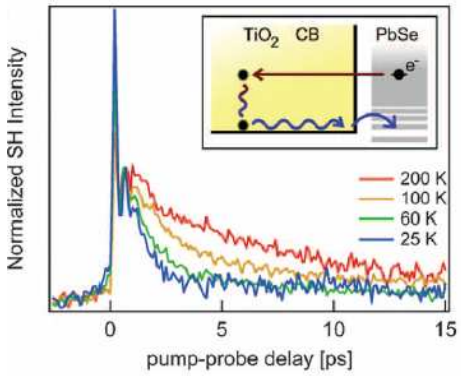


**phonon dynamics 2 - 4 THz**

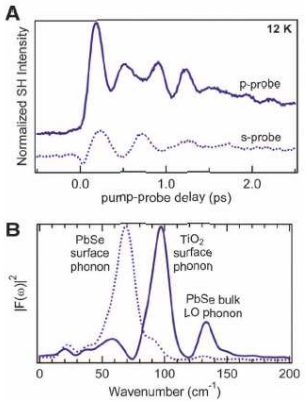


**→ use fs grazing incidence diffraction to study nanoscale depth-resolved carrier & atom dynamics**

# laser-pump / X-ray-probe

# non-resonant hard x-ray diffraction on manganites

**( FEMTO slicing source )**

# Transition Metal Oxides: Complicated Phase Diagrams - Manganites

## Complex phase diagrams reveal the existence of several competing states

[ J.W. Lynn et al., Phys. Rev. B 76 (2007) ]

spin: CE-type & charge/orbital: stripe pattern

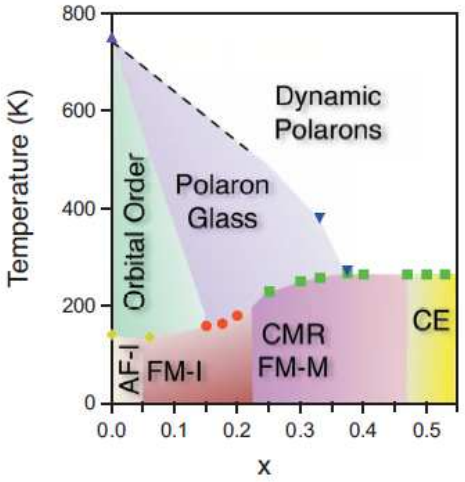


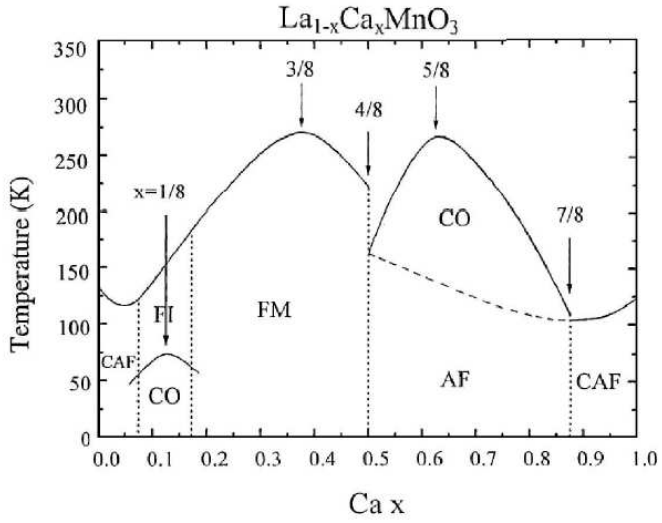


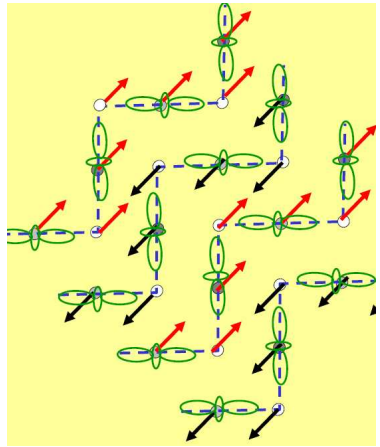

[ H.Y. Hwang & S.-W. Cheong, Monographs in Condensed Matter Science (1999) ]

**Two competing states ($x \sim 0.5$)**

**High T:** Ferromagnetic (FM) Metallic

⇕

**Low T:** Charge-Ordered (CO) & Antiferromagnetic (AFM) Insulating (AFI)

# Complexity in Strongly Correlated Electronic Systems - Manganites

**Complexity: generation of properties that do not preexist in a systems constituent**

**clean limit: two competing phases**

| Transition | HT phase | first order transition | LT phase |
|---|---|---|---|
| Metal-to-Insulator (MIT) | insulating | ⇔ | metallic |
| Magnetic | paramagnetic (PM) | ⇔ | ferromagnetic (FM) |

**quenched disorder: both states are nearly degenerate and coexist**

⇕

**local: PM or FM short-distance correlations ↔ global: neither of the two state dominates**

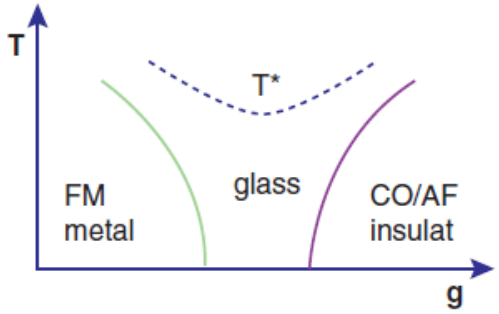


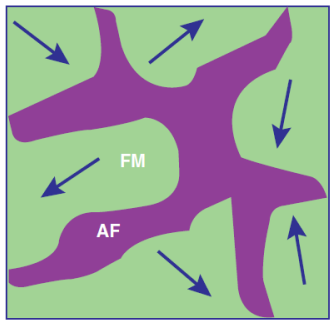


**Generic phase diagram of two competing states: FM metal vs. CO/AF insulator (g is a variable to move from one phase to the other)**

**Sketch of CMR state: FM clusters with randomly oriented moments separated by regions with where a competing CO/AF phase is stabilized**

**[ E. Dagotto, Science 309 (2005) ]**

# Percolation in a Manganite $La_{0.33}Pr_{0.34}Ca_{0.33}MnO_3$ Thin Film

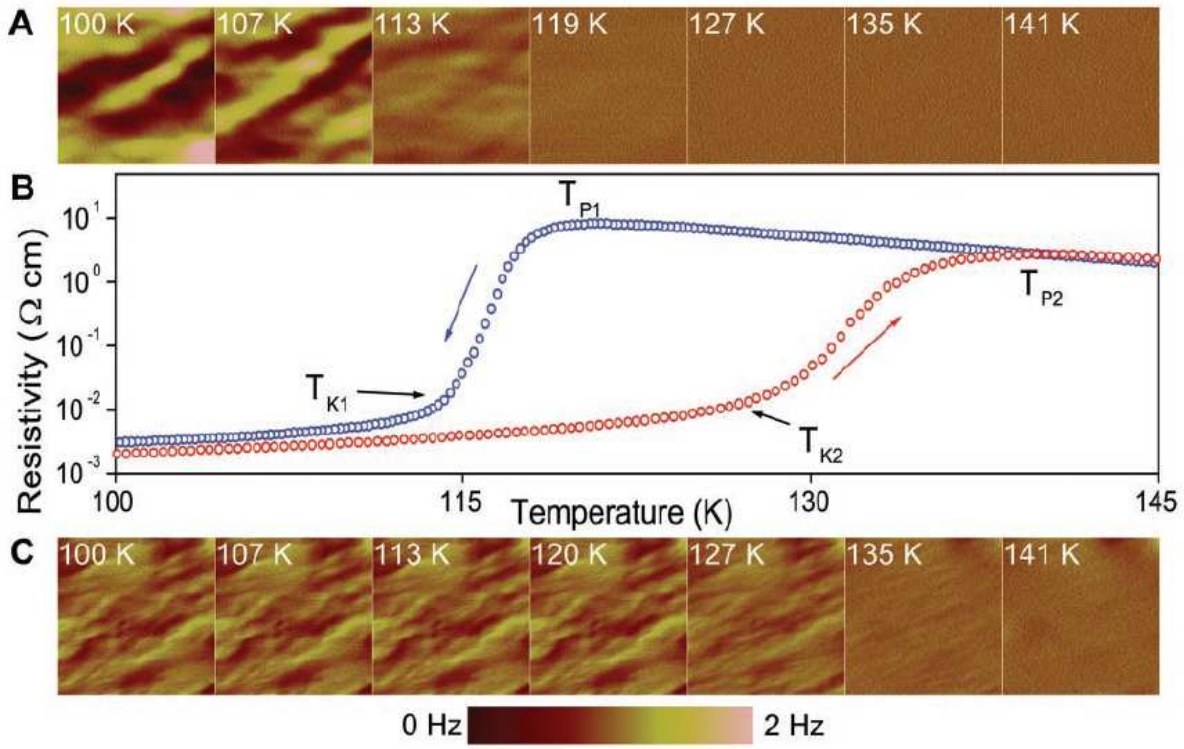


[ L. Zhang et al., Science 298 (2002) ]

**Local magnetic microstructure using low temperature (LT) magnetic force microscope (MFM)**

**Direct observation of inhomogeneity and AFM-FM phase separation upon heating/cooling**

**CMR effect: ground state is a nanoscale mixture of insulating regions and metallic FM domains ?**

[ E. Dagotto, Science 309 (2005) ]

# Manganites: spin-, charge-, orbital- & lattice coupling

[ E. Dagotto, Phys. Rep. 344 (2001) ]

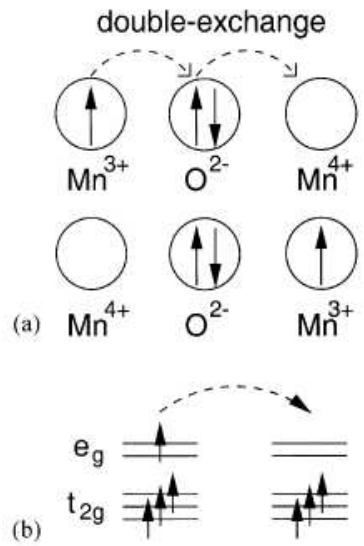


**double exchange mechanism**

**FM - orbital**

**$e_g$ - electron hopping**

**hopping enhanced in FM state**

**spin directions preserved**

[ Y. Tokura, Rep. Prog. Phys. 69 (2006) ]

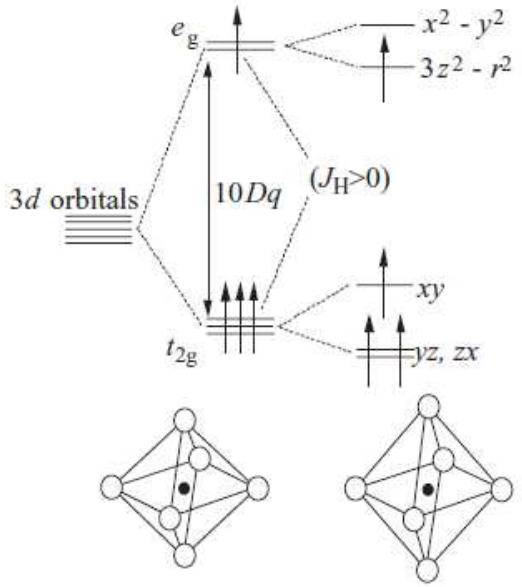


**Jahn-Teller distortion**

**orbital - lattice**

**local distortions at $Mn^{3+}$ site**

**orbital ordering to be considered**

**electron-phonon coupling**

# Orbital-lattice coupling: Jahn-Teller (J-T) distortion of $MnO_6$ octahedron

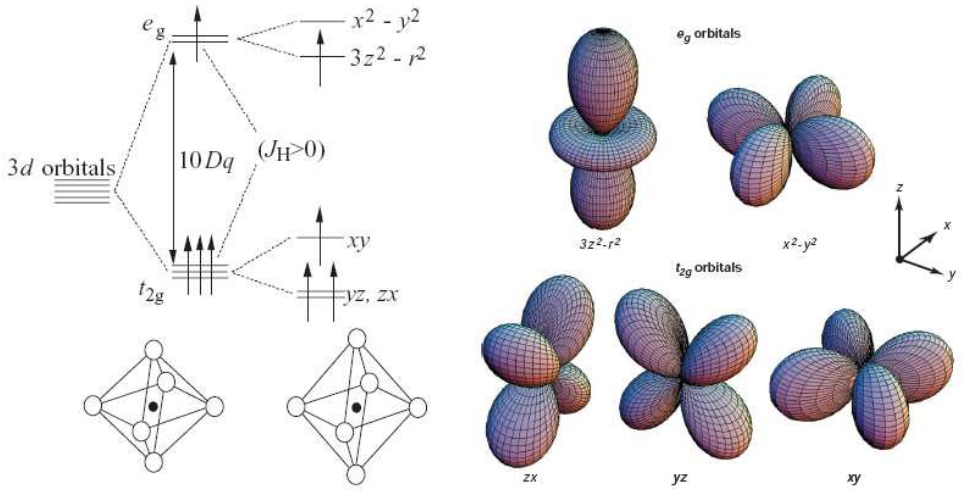


**Crystal-field splitting of the five-fold degenerate 3d levels: 10 Dq $\sim$ 4-5 meV**

**J-T distortion ($\sim$ 1-2 meV) lifts $t_{2g}$ and $e_g$ degeneracy causing $MnO_6$ deformation**

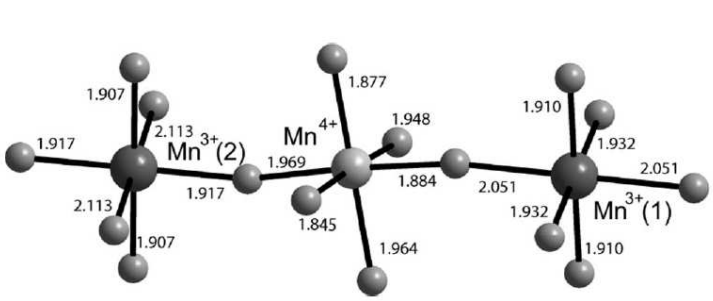


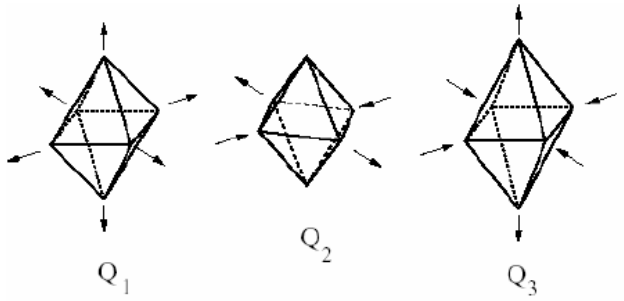


**Local structure of $La_{0.5}Ca_{0.5}MnO_3$** [E.E. Rodriquez et al., PRB 71 (2005)]

**The active J-T modes of the oxygen octhedra, couple with the $e_g$ orbitals**

# Photoinduced J-T Release at $Mn^{3+}$ Site $\Rightarrow$ Change of Crystal Symmetry

**20 K : cell doubling**

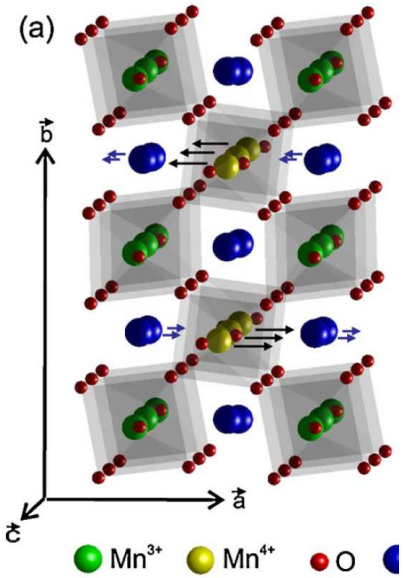


**$(5\bar{5}2)$ superlattice reflection**

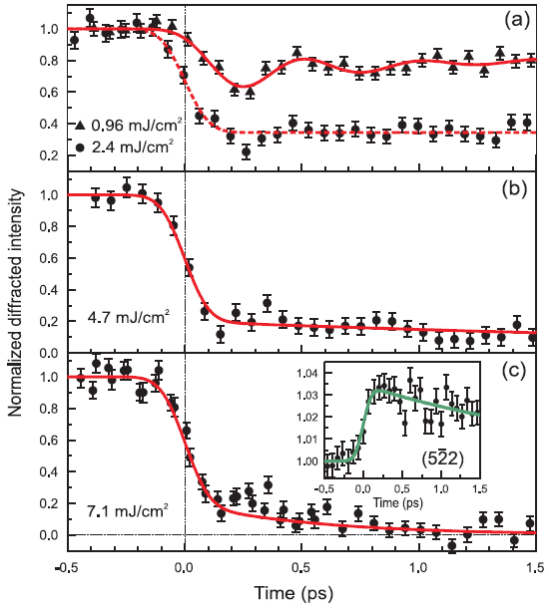


**300 K**

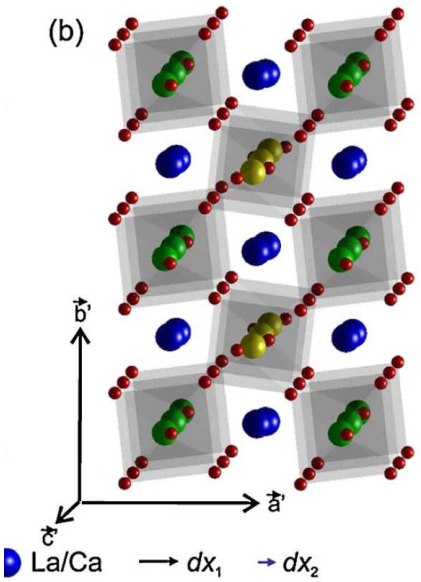


**laser excitation: 1.55 eV**

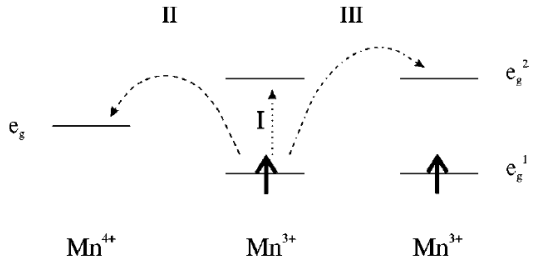


[P. Beaud et al., Phys. Rev. Lett. 103 (2009)]

[J.H. Jung et al., PRB 57 (1998)]

**Mn 3d - O 2p hybridization allows (dipole forbidden) intra-atomic transition $e_g^1(Mn^{3+}) \rightarrow e_g^1(Mn^{3+})$**

# $La_{1-x}Ca_xMnO_3$: Dynamics at Short (fs) & Long (ps - ns) Time Scales

- **Short time scale:** SL peak drops 80% after 200 fs (= time resolution) and $\sim$ 100% after 1 ps
- At 1 mJ/cm$^2$ displacive excitation of 2 THz coherent optical phonon (due to La/Ca atom motion)
- Coherent phonon modes of oxygen octahedra drive structural phase transition

  (time scale of structural phase transition set by quarter period of phonon mode)
- Octahedra phonon modes (50 - 70 fs) require time resolution $<$ 10 fs ($\rightarrow$ XFEL)
- Melting of charge & orbital order on time scale $<<$ 100 fs: soft X-ray resonant diffraction ($\rightarrow$ XFEL)

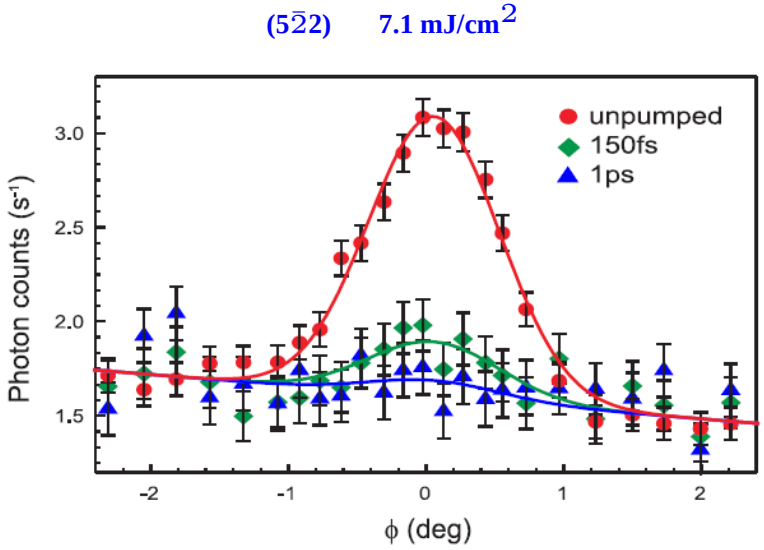


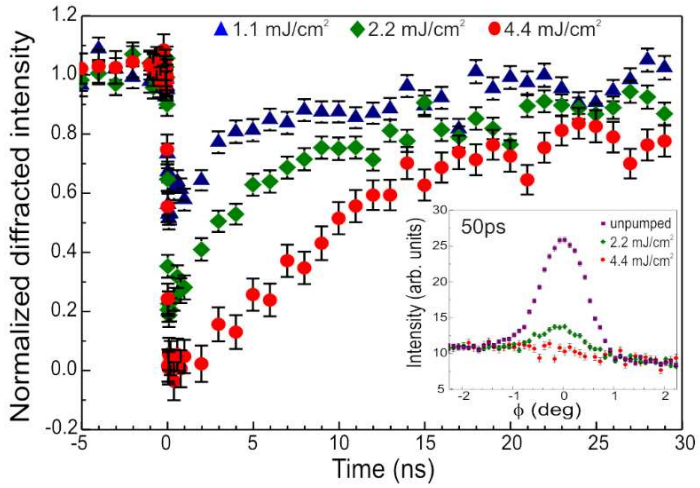


- **Long time scale:** ground state recovers completely after 100 ns allowing stroboscopic measurements

  Drop from 70% (200 fs) $\rightarrow$ 50% (50 ps) at 1 mJ/cm$^2$ indicates 'thermal' formation of coexisting ordered & disordered domains on a ps time scale

# laser-pump / X-ray-probe

# resonant soft x-ray diffraction on multiferroic

**( LCLS free electron laser )**

# Resonant X-Ray Diffraction (RXRD): Charge-, Orbital- & Magnetic Order

**Tunability:** energy tuned to absorption edges

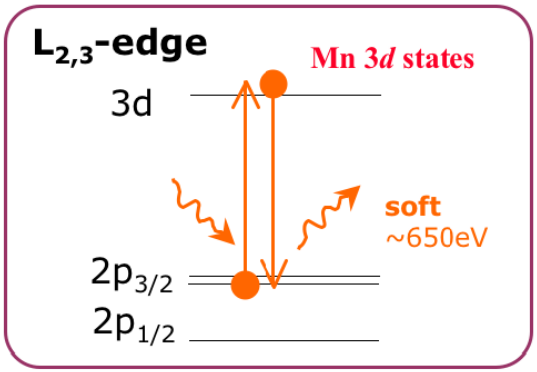


**Resonant process:** intermediate states

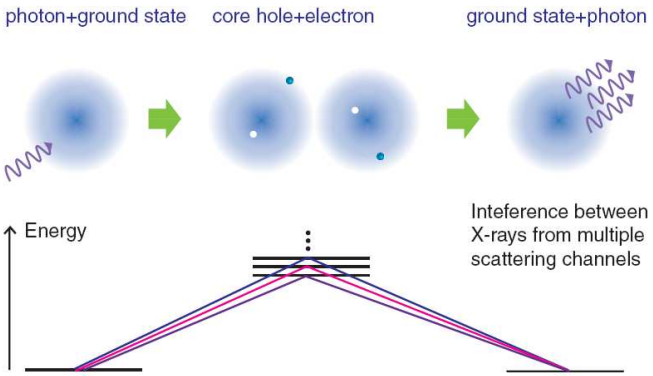


**Coherent summation:** interference

$$F \propto \left\langle \mathbf{T}_q^k \right\rangle \propto \sum_n \frac{\langle g|O|n\rangle\langle n|O^*|g\rangle}{E_n - E_g - \hbar\omega + i\Gamma}$$

**Sensitive to both:**

- **O 2p - Mn 3d overlap**
- **orbital ordering / Jahn-Teller**

**Flexible polarization:** multipole decomposition

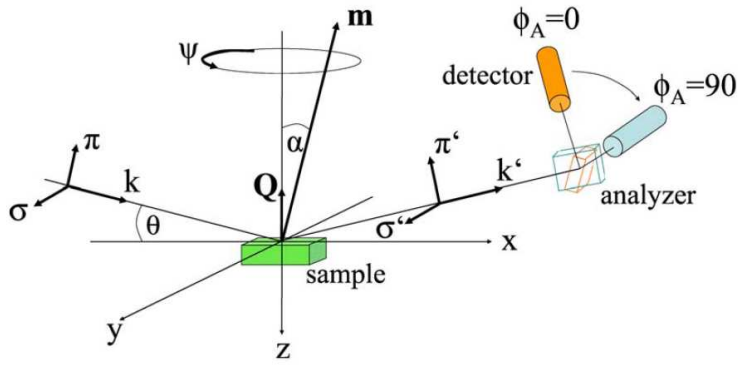

# CuO Resonant Soft X-Ray Scattering: LCLS Collaboration

## Experiment

**FEMTO:**
S. L. Johnson (PI)
E. Vorobeva
P. Beaud
A. Caviezel
G. Ingold

**RESOX:**
U.Staub
R. De Souza
V. Scagnoli

**External:**
M. Trigo (SLAC)
A. T. Boothroyd (Oxford)

## Beamline

W. Schlotter
J. Turner

## Endstation

W.-S. Lee (Stanford)
Y.-D. Chuang (LBNL)
L. Patthey (PSI/SLS)
R. G. Moore (Stanford)
D. Lu (Stanford)
M. Yi (Stanford)
P. Kirchmann (Stanford)
P. Denes (LBNL)
D. Doering (LBNL)
Z. Hussain (LBNL)
Z. X. Shen (Stanford)

# CuO: A High-T Induced Multiferroic [ Kimura et al., Nat. Mat. 7 (2008) ]

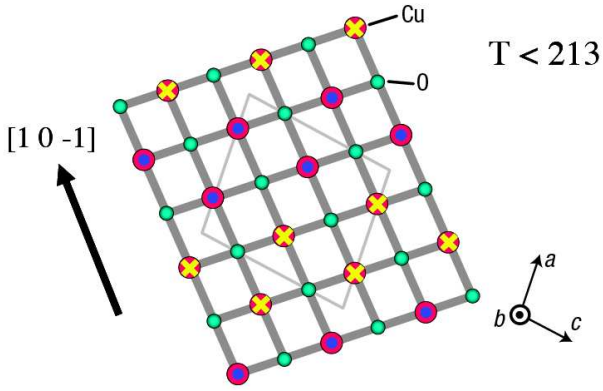


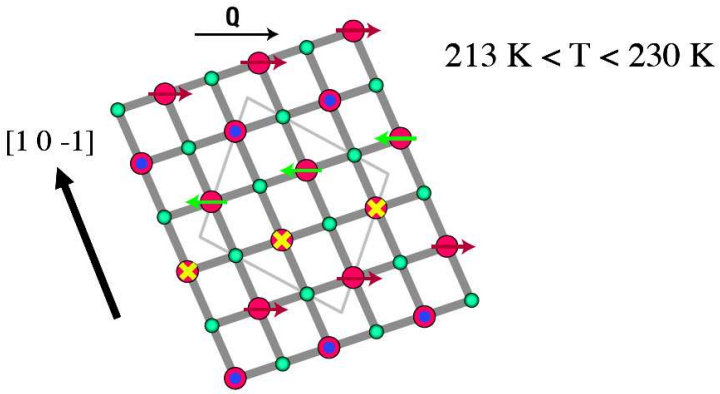


**Low T: collinear antiferromagnetic order**

**non-multiferroic, commensurate, $q_{CM}$=(0.5 0 -0.5)**

**High T: spiral magnetic order**

**multiferroic, incommensurate, $q_{ICM}$=(0.506 0 -0.483)**

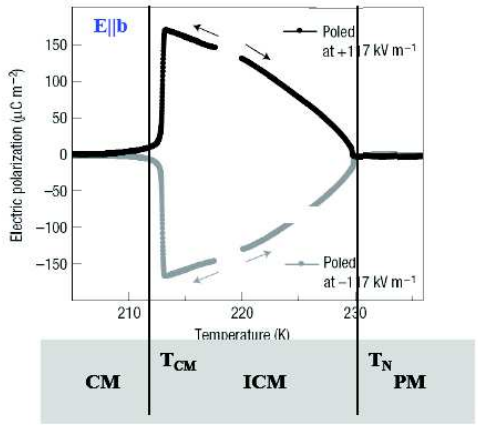


**spontaneous electric polarization**

# CuO: Resonant Soft X-ray Magnetic Scattering (Static)

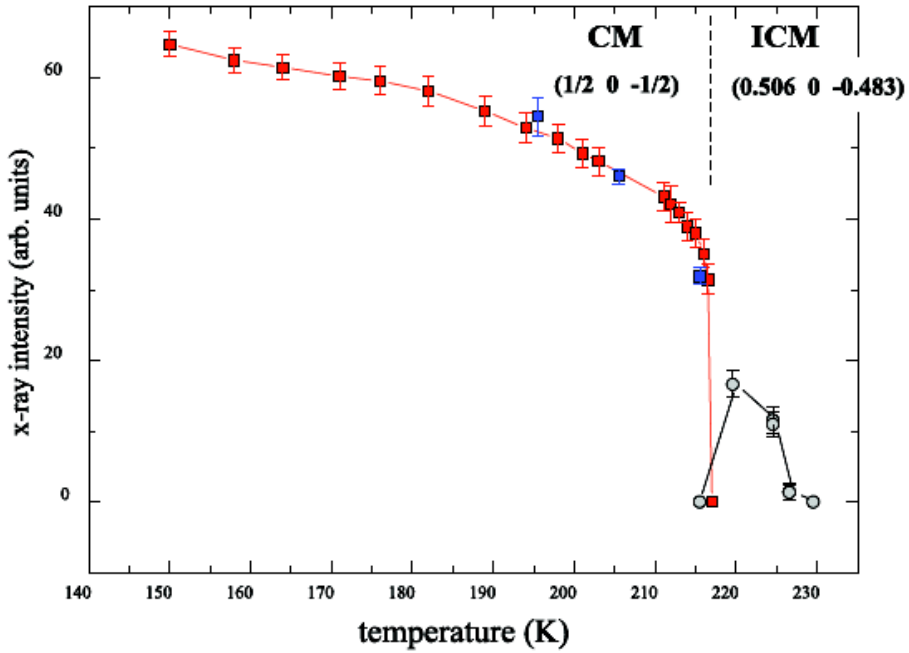


**( RESOXS station at SLS )**

**Temperature dependence: ICM rises as magnetic structure factor decreases ↔ thermal disorder increases**

# LCLS Endstation: Resonant Soft X-Ray Scattering (RSXS)

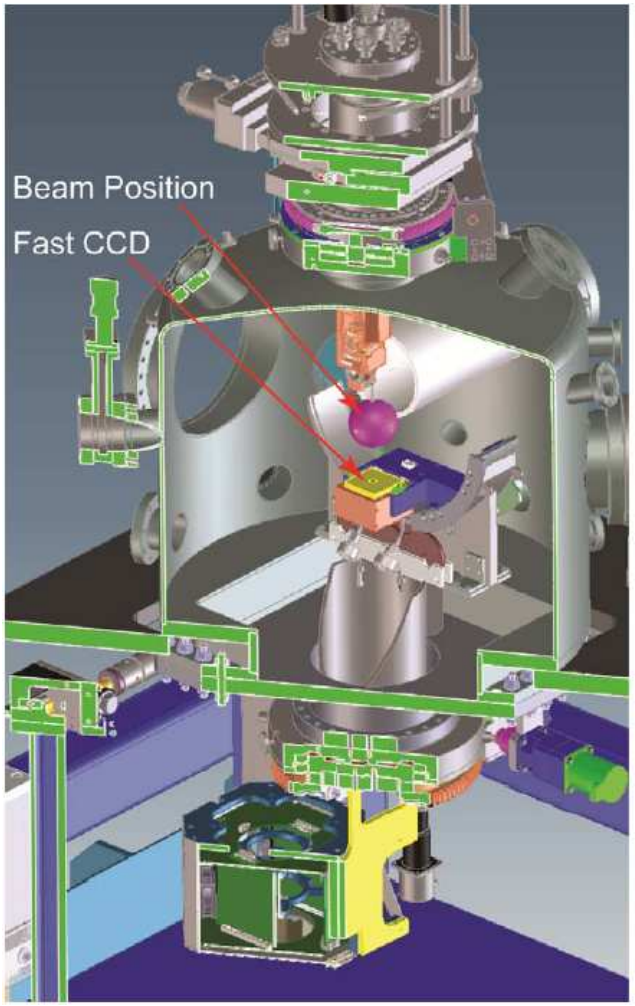


1. **APD/Channeltrons:**
   - Diagnostic XAS
   - Point detector
2. **Fast 2-D CCD detector (FCCD):**
   - Developed by LBNL.
   - **200 frames per sec. ->Pulse-by-pluse data collection.**
   - 480 by 480 array of 30 μm square pixels
   - 8° acceptance, 0.017° per pixel.
3. **Two-level CCD detector backup plan.**

LBNL Fast CCD

**Successfully tested at the ALS for soft x-ray use.**

**For LCLS experiment: Necessary to operate in-vacuum with 2 degrees of rotations.**

**[ constructed by consortium: LBL - DESY - SLAC ]**

# Femtosecond Magnetic Order Dynamics in Multiferroic CuO

**Pump-probe RXRD experiment at Cu $L_3$ edge 930 eV (SXR instrument at LCLS)**

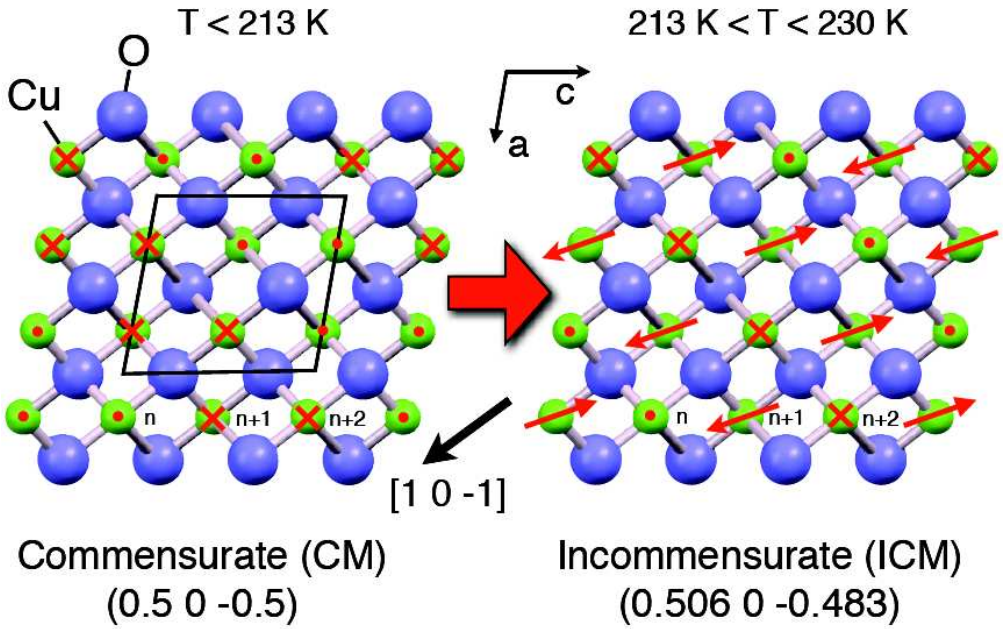


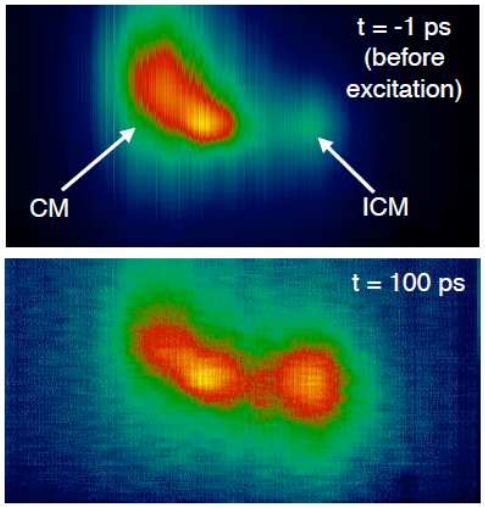


**Magnetic phase transition: CM collinear AFM ⇒ ICM spiral AFM magnetic ordering**

[ S.L. Johnson et al., arXIV:1106.6128v1 (2011) ]

(collaboration: PSI - U Stanford - LBL - SLAC - XFEL - U Oxford)

# Magnetic Order Dynamics in CuO: Time-Dependence of Ratio $I_{CM}/I_{ICM}$

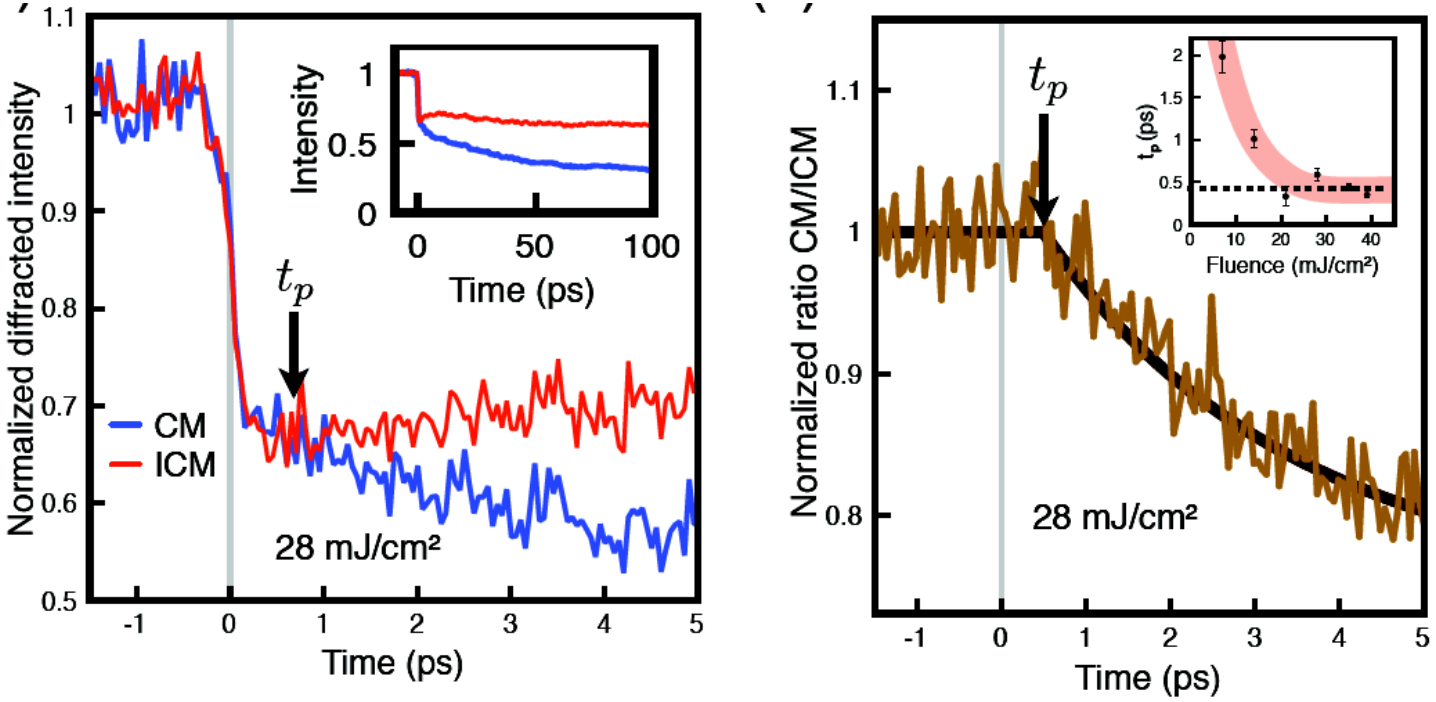


- Sudden drop for both peaks, difference after time $t_p$ due to shift in population of the CM and ICM domains

- Limiting time scale of $t_p$ $\sim$ 400 fs corresponding to 1/4 coherent oscillation of a low momentum $q \sim 0$ spin wave

# Antiferromagnetic Phase Transition Driven by Disorder: CuO chain

[ D.A. Yablonskii, Physica C 171 (1990) ]

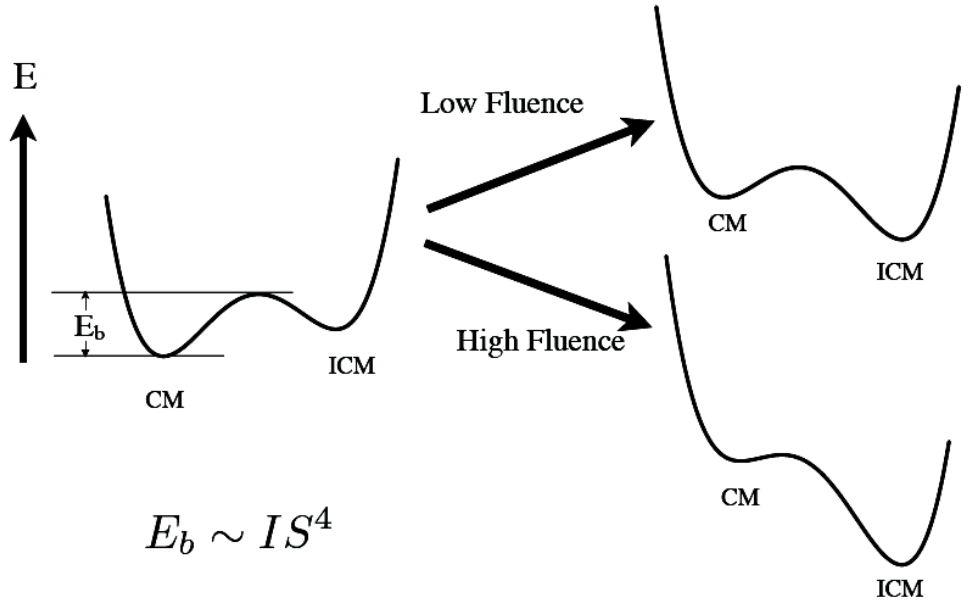


$$E_b \sim IS^4$$

$$E = \sum_n [J_1 \mathrm{S}_n \mathrm{S}_{n+1} + J_2 \mathrm{S}_n \mathrm{S}_{n+2} + I(\mathrm{S}_n \mathrm{S}_{n+1})(\mathrm{S}_{n+1} \mathrm{S}_{n+2})]$$

**Exchange interactions:** $J_1 < 0$: nearest neighbor FM; $J_2 > 0$: next-nearest neighbor AFM; $I > 0$: biquadratic term

**spins:** $\mathrm{S}_n$ : spin of Cu atom along the c-axis; $S$: spatially averaged value of spin magnitude

$S^2 > J_1^2/8IJ_2$: $\mathrm{E}_{CM} < \mathrm{E}_{ICM}$, but S decreases with temperature $\rightarrow S^2 < J_1^2/8IJ_2$ and $\mathrm{E}_{ICM} < \mathrm{E}_{CM}$

# Summary & conclusions (1): fs laser-pump / X-ray-probe

- Coherent modes can launch non-equilibrium phase transition in solids on a fs time scale

  → Structural phase transition: coherent phonon excitation (experiment at Slicing Source)

  → Magnetic phase transition: coherent spin wave (magnon) excitation (experiment at XFEL)

- Fundamental time scale: quarter/half period of coherent phonon/magnon oscillation

- Laser slicing sources provide valuable proof-of-principle experiments prior to XFELs

- Time resolution achieved in experiments: 100 - 200 fs (slicing sources) & 250 - 350 fs (XFELs)

- But: we need time resolution $< 10$ fs !

- Pump-probe experiments on correlated systems are feasible at XFELs

- fs probing of long-range electronic-, spin- and atomic order in solids:

  → fs non-resonant and resonant X-ray scattering in soft & hard X-ray regime demonstrated

- XFEL experiments need careful preparation

  → all optical pump-probe & static x-ray experiments (i.e. reflectivity, MOKE, static RESOXS, etc.)

- We just started ... much work lies ahead:

  → short pulses, timing, flexible pumping schemes, flexible polarization, flexible sample environment, fully coherent beams, coherent diffraction, ...

# Summary & conclusion (2): fs laser-pump / X-ray-probe

**To resolve the correlated dynamics between lattice, charge, orbital and spin in complex materials in real time with femtosecond x-ray diffraction, we need . . .**

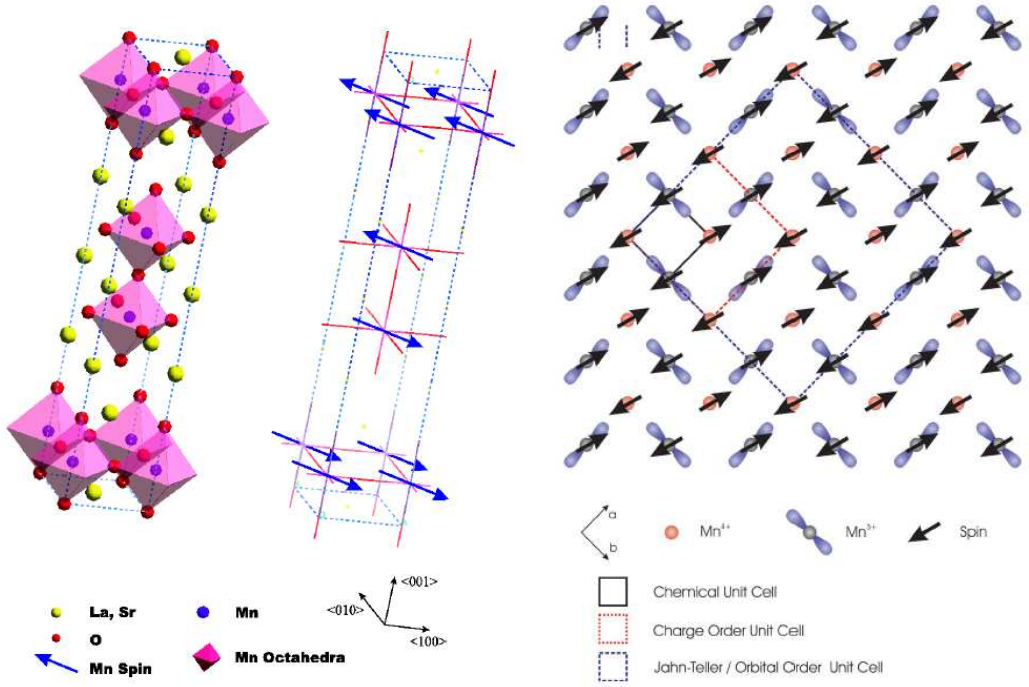


**. . . 10 - 100 fs FWHM soft $\oplus$ hard x-rays & flux on sample $\sim 10^8$ ph/pulse/0.1% bw (focus 10 x 10 $\mu\mathrm{m}^2$) & lin $\oplus$ circ polarization & pump-probe timing jitter $\leq$ 10 fs FWHM**